

## Deep learning for neuroimaging-based diagnosis and rehabilitation of Autism Spectrum Disorder: A review

Marjane Khodatars<sup>a</sup>, Afshin Shoeibi<sup>b,c, \*\*</sup>, Delaram Sadeghi<sup>a</sup>, Navid Ghaasemi<sup>b,c</sup>, Mahboobeh Jafari<sup>d</sup>, Parisa Moridian<sup>e</sup>, Ali Khadem<sup>f,\*</sup>, Roohallah Alizadehsani<sup>g</sup>, Assef Zare<sup>h</sup>, Yinan Kong<sup>i</sup>, Abbas Khosravi<sup>g</sup>, Saeid Nahavandi<sup>g</sup>, Sadiq Hussain<sup>j</sup>, U. Rajendra Acharya<sup>k,l,m</sup>, Michael Berk<sup>n,o</sup>

<sup>a</sup> Dept. of Medical Engineering, Mashhad Branch, Islamic Azad University, Mashhad, Iran

<sup>b</sup> Faculty of Electrical Engineering, FPGA Lab, K. N. Toosi University of Technology, Tehran, Iran

<sup>c</sup> Computer Engineering Department, Ferdowsi University of Mashhad, Mashhad, Iran

<sup>d</sup> Electrical and Computer Engineering Faculty, Semnan University, Semnan, Iran

<sup>e</sup> Faculty of Engineering, Science and Research Branch, Islamic Azad University, Tehran, Iran

<sup>f</sup> Department of Biomedical Engineering, Faculty of Electrical Engineering, K. N. Toosi University of Technology, Tehran, Iran

<sup>g</sup> Institute for Intelligent Systems Research and Innovation (IISRI), Deakin University, Victoria, 3217, Australia

<sup>h</sup> Faculty of Electrical Engineering, Gonabad Branch, Islamic Azad University, Gonabad, Iran

<sup>i</sup> School of Engineering, Macquarie University, Sydney, 2109, Australia

<sup>j</sup> Dibrugarh University, Assam, 786004, India

<sup>k</sup> Ngee Ann Polytechnic, Singapore, 599489, Singapore

<sup>l</sup> Dept. of Biomedical Informatics and Medical Engineering, Asia University, Taichung, Taiwan

<sup>m</sup> Dept. of Biomedical Engineering, School of Science and Technology, Singapore University of Social Sciences, Singapore

<sup>n</sup> Deakin University, IMPACT – the Institute for Mental and Physical Health and Clinical Translation, School of Medicine, Barwon Health, Geelong, Australia

<sup>o</sup> Orygen, The National Centre of Excellence in Youth Mental Health, Centre for Youth Mental Health, Florey Institute for Neuroscience and Mental Health and the Department of Psychiatry, The University of Melbourne, Melbourne, Australia

### ARTICLE INFO

#### Keywords:

Autism spectrum disorder  
Diagnosis  
Rehabilitation  
Deep learning  
Neuroimaging  
Neuroscience

### ABSTRACT

Accurate diagnosis of Autism Spectrum Disorder (ASD) followed by effective rehabilitation is essential for the management of this disorder. Artificial intelligence (AI) techniques can aid physicians to apply automatic diagnosis and rehabilitation procedures. AI techniques comprise traditional machine learning (ML) approaches and deep learning (DL) techniques. Conventional ML methods employ various feature extraction and classification techniques, but in DL, the process of feature extraction and classification is accomplished intelligently and integrally. DL methods for diagnosis of ASD have been focused on neuroimaging-based approaches. Neuroimaging techniques are non-invasive disease markers potentially useful for ASD diagnosis. Structural and functional neuroimaging techniques provide physicians substantial information about the structure (anatomy and structural connectivity) and function (activity and functional connectivity) of the brain. Due to the intricate structure and function of the brain, proposing optimum procedures for ASD diagnosis with neuroimaging data without exploiting powerful AI techniques like DL may be challenging. In this paper, studies conducted with the aid of DL networks to distinguish ASD are investigated. Rehabilitation tools provided for supporting ASD patients utilizing DL networks are also assessed. Finally, we will present important challenges in the automated detection and rehabilitation of ASD and propose some future works.

### 1. Introduction

ASD is a disorder of the nervous system that affects the brain and

results in difficulties in speech, social interaction and communication deficits, repetitive behaviors, and delays in motor abilities [1]. This disease can generally be distinguished with extant diagnostic protocols

\* Corresponding author. Department of Biomedical Engineering, Faculty of Electrical Engineering, K. N. Toosi University of Technology, Tehran, Iran.

\*\* Corresponding author. Faculty of Electrical Engineering, FPGA Lab, K. N. Toosi University of Technology, Tehran, Iran.

E-mail addresses: [Afshin.shoeibi@gmail.com](mailto:Afshin.shoeibi@gmail.com) (A. Shoeibi), [alikhadem@kntu.ac.ir](mailto:alikhadem@kntu.ac.ir) (A. Khadem).

from the age of three years onwards. ASD influences many parts of the brain. This disorder also involves a genetic influence via the gene interactions or polymorphisms [2,3]. One in 70 children worldwide is affected by ASD. In 2018, the prevalence of ASD was estimated to occur in 168 out of 10,000 children in the United States, one of the highest prevalence rates worldwide. ASD is significantly more common in boys than in girls. In the United States, about 3.63% of boys aged 3–17 years have ASD, compared with approximately 1.25% of girls [4–6].

In the past, ASD was divided into five groups: Asperger's syndrome (AS) [7], Rett syndrome (RS) [8], childhood disintegrative disorder (CDD) [9], autistic disorder (classic autism) [10], and pervasive developmental disorder – not otherwise specified (PDD-NOS) [11]. Diagnostic and statistical manual of mental disorders, 5th Edition (DSM-5) is a book published by the American psychiatric association (APA) for the classification of mental disorders using common language and standard criteria [12]. The book was approved by the APA board of trustees on December 1, 2012 and published on May 18, 2013. Significant changes to the DSM-5 has been made to autism to include the removal of subtypes of autism, namely Asperger's syndrome, classic autism, RS, PDD-NOS, and their placement under an umbrella called ASD [13]. The severity level of ASD is determined on a spectrum that includes 3 levels of severity: level 1: needs support, level 2: needs substantial support, and level 3: needs very substantial support [13]. [Figure \(1\)](#) shows the distribution map of ASD throughout the world [14]. [Figure \(2\)](#) shows the visualization of different levels of ASD [15].

No certain treatment has been presented for ASD, but various intervention techniques have been studied and developed to decrease the symptoms, improve the cognitive ability, improve daily life skills, and increase the capabilities of ASD patients. Various intervention approaches are used for the patients suffering from ASD, where most of them are based on behavioral approaches, and some of them are based on evolutionary/cognitive approaches [16].

In recent years, noninvasive brain stimulation (NIBS) methods [17], including transcranial direct current stimulation (tDCS) [18] and transcranial magnetic stimulation (TMS) [19], have been examined as new treatment alternatives for modifying pathological neuroplasticity in ASD disorders [17]. tDCS is a non-invasive brain stimulation method

that employs direct electric currents to stimulate certain parts of the brain [18]. Also, TMS is a non-invasive brain stimulation method based on electromagnetic induction that concentrates on the brain areas that play an essential role in adjusting the behavior of ASD patients [19].

ASD diagnosis methods include various tools used by psychologists, specialists, and facilitators [20]. The tests are autism diagnostic observation schedule 2nd edition (ADOS-2) [21], autism diagnostic interview-revised (ADI-R) [22], childhood autism rating scale (CARS) [23], diagnostic interview for social and communication disorder (DISCO) [24], Gilliam autism rating scale (GARS) [25], developmental, dimensional, and diagnostic interview (3di) [26] and modified checklist for autism in toddlers (M-CHAT) [27]. These methods are mainly interview-based, with the advantage that interviews can be easily done for all ages [28]. The interview-based methods have few disadvantages [29]. The major shortcoming of these methods is that they are subjective. The diagnosis of the disease depends on the physician's expertise, skill, and schedule. Another disadvantage of the interview-based methods is that the child's family members may not be honest in filling the questionnaire or answering the questions, which may result in an incorrect diagnosis [30].

Neuroimaging techniques are another class of ASD diagnosis methods that are preferred by specialists. In the recent decade, various investigations for the diagnosis of ASD have been conducted on neuroimaging data (structural and functional). Analyzing anatomy and structural connections of brain areas with structural neuroimaging is an essential tool for studying structural disorders of the brain in ASD. The principal tools for structural brain imaging are magnetic resonance imaging (MRI) techniques [31–33].

Cerebral anatomy is investigated by structural MRI (sMRI) images and anatomical connections are assessed by diffusion tensor imaging MRI (DTI-MRI) [34]. Investigating the activity and functional connections of brain areas using functional neuroimaging can also be used for studying ASD. Brain functional diagnostic tools are more primary approaches than structural methods for studying ASD.

The most basic modality of functional neuroimaging is electroencephalography (EEG), which records the electrical activity of the brain from the scalp with a high temporal resolution (in milliseconds order)

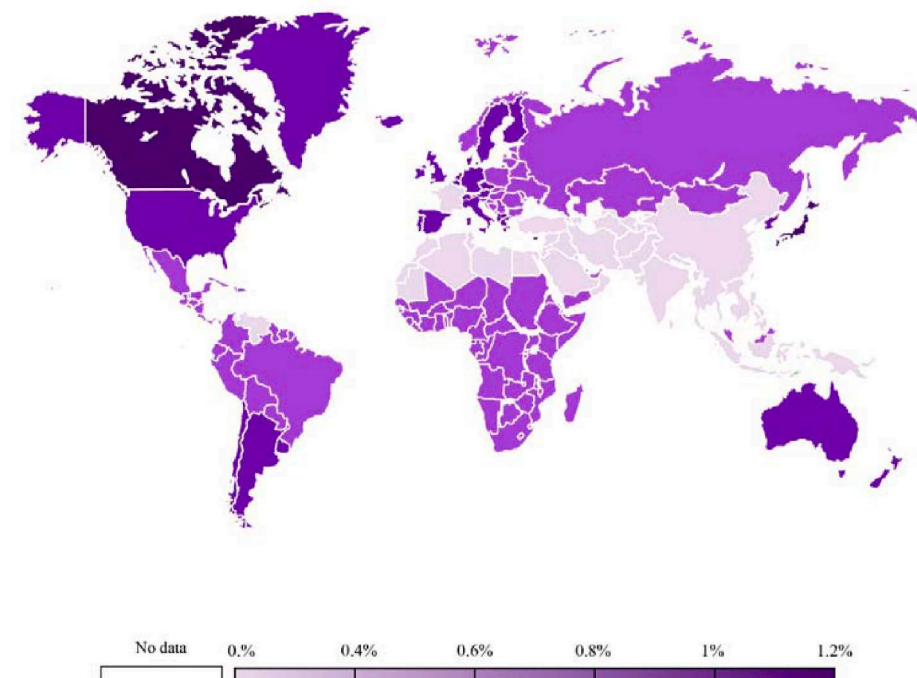


[Fig. 1.](#) Distribution map of ASD throughout the world [14].

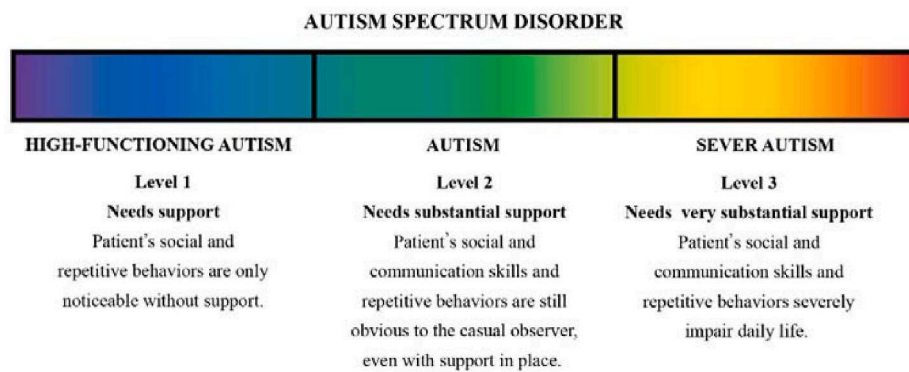


**Fig. 2.** Visualization of different levels of ASD [15].

[35]. Studies have shown that employing EEG signals to diagnose ASD have been useful [36–38]. Functional MRI (fMRI) is one of the most promising imaging modalities in functional brain disorders, used as task-based (T-fMRI) or resting-state (rs-fMRI) [39,40]. fMRI-based techniques have a high spatial resolution (in the order of millimeters) but a low temporal resolution due to slow response of the hemodynamic system of the brain as well as fMRI imaging time constraints and is not ideal for recording the fast dynamics of brain activities. In addition, these techniques have a high sensitivity to motion artifacts. It should be stressed that in consonance with studies, three less prevalent modalities of electrocorticography (ECOG) [41], functional near-infrared spectroscopy (fNIRS) [42], and Magnetoencephalography (MEG) [43] can also attain reasonably performance in ASD diagnosis.

An appropriate approach is to utilize machine-learning techniques alongside functional and structural data to collaborate with physicians in the process of accurately assessing ASD. In the field of ASD, applying machine learning methods generally entail two categories of traditional methods [44] and DL methods [45]. As opposed to traditional methods, much less work has been done on DL methods to explore ASD or design rehabilitation tools.

In this review, IEEE Xplore, ScienceDirect, SpringerLink, ACM, as well as other conferences or journals were used to acquire papers on ASD diagnosis and rehabilitation using DL methods. Further, the keywords "ASD", "Autism Spectrum Disorder" and "Deep Learning" were used to select the papers. The papers are analyzed until November 08th, 2020 by the authors. Figure (3) depicts the number of considered papers using DL methods for the automated detection and rehabilitation of ASD each year.

This study reviews assessment and rehabilitation of ASD patients with DL networks. The outline of this paper is as follows. Section 2 presents the DL networks employed for automated detection of ASD. In section 3, various available public datasets and brief description of various DL models used for ASD are presented. In section 4, DL-based rehabilitation tools for supporting ASD patients are introduced.

Section 5 reveals the challenges of ASD diagnosis and rehabilitation using DL techniques. The state-of-the-techniques proposed to detect ASD accurately are discussed in section 6. The future works are described in section 7 and finally paper concludes in section 8.

## 2. Deep learning techniques for ASD diagnosis and rehabilitation

Nowadays, DL algorithms are used in many areas of medicine, including structural and functional neuroimaging. The application of DL in neural imaging ranges from brain MR image segmentation [46], to the detection of brain lesions such as tumors [47], diagnosis of the brain functional disorders such as ASD [48], and production of artificial structural or functional brain images [49]. Machine learning techniques, based on the type of feedback they need for training, are categorized into three fundamental categories of learning: supervised learning [50], unsupervised learning [51], and reinforcement learning (RL) [52]. DL methods have been applied for nearly all of these categories; so far, most studies applied to identify ASD using DL have been based on supervised or unsupervised approaches. Figure (4) illustrates generally employed types of DL networks, organized by their underlying structure, to study ASD.

## 3. CADS-based deep learning techniques for ASD diagnosis by MRI modalities

A traditional AI-based CADS encompasses several stages of data acquisition, data pre-processing, feature extraction, and classification [53–56]. In [57–59] existing traditional algorithms for diagnosing ASD have been reviewed. In contrast to traditional methods, in DL-based CADS, feature extraction, and classification are performed intelligently within the model. Also, due to the structure of DL networks, using large dataset to train DL networks and recognize intricate patterns in datasets is incumbent. The components of DL based CADS for ASD detection are

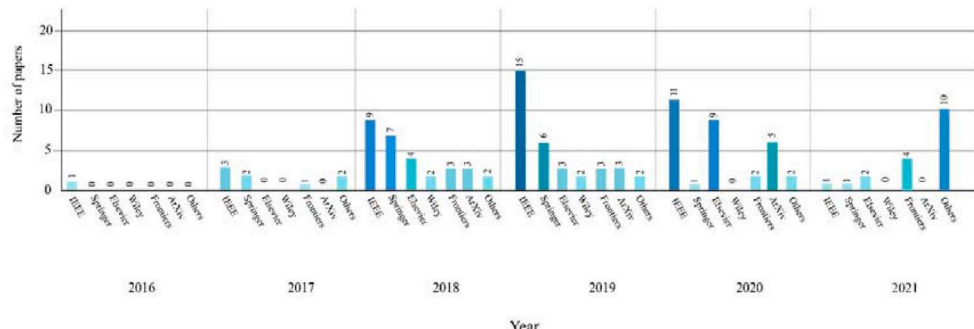


**Fig. 3.** Number of papers published every year for ASD diagnosis and rehabilitation.

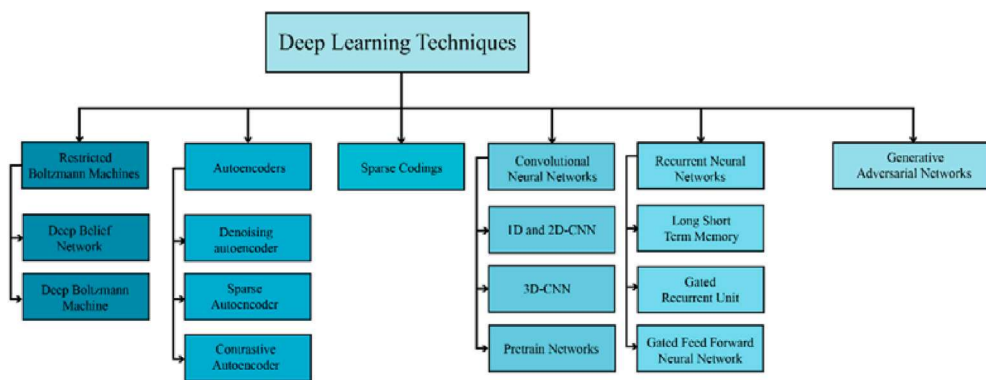


**Fig. 4.** Illustration of various types of DL methods.

shown in [Figure \(5\)](#). It can be noted from the figure that, large and free databases are first introduced to diagnose ASD. In the second step, various types of pre-processing techniques are used on functional and structural data to be scrutinized. Finally, the DL networks are applied to the preprocessed data.

### 3.1. Neuroimaging ASD datasets

#### 3.1.1. ABIDE dataset

Datasets are the heart of any CADS development, and the capability of CADS depends primarily on the affluence of the input data. To diagnose ASD, several brain functional and structural datasets are available. The most complete free dataset available is ABIDE [60] dataset with two subsets: ABIDE-I and ABIDE-II, which encompasses sMRI, rs-fMRI, and phenotypic data. ABIDE-I involves data from 17 international sites, yielding a total of 1112 datasets, including 539 individuals with ASD and 573 healthy individuals (ages 6–47). In accordance with HIPAA guidelines and 1000 FCP/INDI protocols, these data are anonymized. In contrast, ABIDEII contains data from 19 international sites, with a total of 1114 datasets from 521 individuals with ASD and 593 healthy individuals (ages 5–64). Also, preprocessed images of the ABIDE-I series called PCP [61] can be freely downloaded by the researchers. The second recently released ASD diagnostic database is called NDAR, which comprises various modalities, and more information is provided in [62].

#### 3.1.2. EEG available dataset

This EEG dataset has been presented by King Abdulaziz University (KAU) Brain Computer Interface (BCI) Group, Jeddah, Saudi Arabia which includes a total of 18 files, where 8 files are associated with the disorders group and 10 files belong to the normal group. The disorder group comprises of 8 boys (10–16 years), and the normal group consists of 10 boys (9–16 years). The EEG records were taken in the resting state without artifacts. EEG with a sampling rate of 256 Hz was obtained using active electrodes, active digital EEG amplifier, and BCI2000 recording system. The recording system contained g.tec EEGcap, 16 Ag/AgCl electrodes, g.tec GAMMAbox, g.tec USBamp and BCI2000. While recording, data was filtered using a band-pass filter with the frequency band of 0.1–60 Hz and sampled with a frequency of 256 Hz. The notch filter was also applied to remove power-line noise [63,64].

### 3.2. Preprocessing techniques

Neuroimaging data (especially functional ones) is of relatively complicated structure, and if not pre-processed properly, it may affect the final diagnosis. Preprocessing of this data typically entails multiple common steps performed by different software as standard. Indeed, occasionally prepared pipelines are applied to the dataset to yield pre-processed data for future researches. In the following section, preprocessing steps are briefly explained for fMRI data.

#### 3.2.1. Standard (low-level) fMRI preprocessing steps

Low-level pre-processing of fMRI images normally has fixed number of steps applied to the data, and prepared toolboxes are usually used to reduce execution time and yield better accuracy. Some of these reputable toolboxes are FMRIB software libraries (FSL) [65], BET [66], FreeSurfer [67], and SPM [68]. Also, important and vital fMRI pre-processing incorporates brain extraction, spatial smoothing, temporal filtering, motion correction, slice timing correction, intensity normalization, and registration to the standard atlas, which are summarized as follows:

##### (1). Brain extraction

Brain extraction is the process of removing non-brain tissues like eyes, ears, and skull from the MRI data to obtain a clear image of the brain [69–71]. It is an essential step in the structural analysis that require brain segmentation and functional analyses of brain activity, in which a clear and accurate image of the brain would be obtained. It is implemented in processing toolboxes such as FSL and FreeSurfer [69–71].

##### (2). Spatial smoothing

Involves averaging the adjacent voxels signal. This process is persuasive on account of neighboring brain voxels being usually closely related in function and blood supply [69–71].

##### (3). Temporal filtering

The aim is to eliminate unwanted components from the time series of

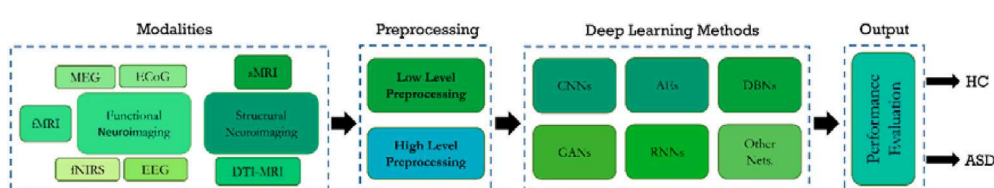


**Fig. 5.** Block diagram of CAD system using DL architecture for ASD detection.

voxels without impairing the signal of interest [69–71].

#### (4). Realignment (Motion Correction)

During the fMRI test, people often move their heads. The objective of motion correction is to align all images to a reference image so that the coordinates and orientation of the voxels be identical in all fMRI volumetric images [69–71].

#### (5). Slice time correction

The purpose of modifying the slice time is to adjust the time series of the voxels so that all the voxels in each fMRI volume image have a common reference time. Usually, the corresponding time of the first slice recorded in each fMRI volume image is selected as the reference time [69–71].

#### (6). Intensity normalization

In this step, the average intensity of fMRI signals are rescaled to compensate for global deviations within and between the recording sessions [69–71].

#### (7). Registration to a standard atlas

The human brain entails hundreds of cortical and subcortical areas with various structures and functions, each of which is very time consuming and complex to study. To overcome the problem, brain atlases are employed to partition brain images into a confined number of ROIs, following which the meantime series of each ROI can be extracted [72]. ABIDE datasets use a manifold of atlases, including Automated Anatomical Labeling (AAL) [73], Eickhoff-Zilles (EZ) [74], Harvard-Oxford (HO) [75], Talaraich and Tournoux (TT) [76], Dosnenbach 160 [77], Craddock 200 (CC200) [78] and Craddock 400 (CC400) [79] and more information is provided in [80]. Table 1 provides complete information on preprocessing tools, atlases, and some other preprocessing information.

#### (8). Pipeline methods

Pipelines present preprocessed images of ABIDE databases. They embrace generic preprocessing procedures. Employing pipelines, distinct methods can be compared with each other. In ABIDE datasets, preprocessing is performed by four pipeline techniques: neuroimaging analysis kit (NIAK) [161], data processing assistant for rs-fMRI (DPARSF) [162], the configurable pipeline for the analysis of connectomes (CPAC) [163], or connectome computation system (CCS) [164]. The preprocessing steps carried out by the various pipelines are comparatively analogous. The chief differences are in the particular algorithms for each step, the software simulations, and the parameters applied. Details of each pipeline technique are provided in [80]. Table 1 demonstrates the pipeline techniques used in ASD detection exploiting DL.

##### 3.2.2. Standard (low-level) sMRI preprocessing steps

Similar to fMRI preprocessing, structural MR images are also usually preprocessed before feeding to a neural network. Brain extraction and registration to a standard atlas are common steps in both fMRI and sMRI preprocessing. The rest of the steps are described as follows:

#### (1). Denoising

Diagnosis of ASD using sMRI images may confront serious challenges due to the noise resulted from the recording image process. To reduce these noises, there is a wide range of filtering approaches such as low-pass filters, wavelet-based filters, NLM filters, etc. [165].

#### (2). Inhomogeneity correction

The static magnetic field must be homogeneous when recording sMRI data, but in reality, this homogeneity is diminished due to the presence of brain tissues and creates artifact on images. Therefore, Inhomogeneity Correction must be carried out before sMRI image processing. More information is available in [165].

#### (3). Intensity standardization

Generally, sMRI images with contrasts like T1-Weighted, acquired by different scanners have not the same intensity. Intensity standardization techniques in sMRI endeavor to remove these scanner-dependent intensity variations [165]. Most simple approaches to standardize the intensity of sMRI images rely on histogram matching techniques [165].

#### (4). De-oblique

During the sMRI data acquisition, the scan angle occasionally deviates from the horizon to cover the whole brain. This scan is called an oblique scan. Oblique scanning allows data to be acquired with less noise but can make registration between two different images more demanding. To address this problem, the de-oblique preprocessing step is fulfilled [166].

#### (5). Re-orientation

The orientation of sMRI images depends on the settings of the image recording process. In order to process images accurately, all of them must have the same orientation. The orientation of sMRI images encompasses right or left, anterior or posterior, and finally superior or inferior [166].

#### (6). Segmentation:

Sometimes it is imperative to segment sMRI images before applying high-level processing. In sMRI modalities, segmentation of brain images usually aims to isolate three types of brain tissues: white matter (WM), gray matter (GM), and cerebrospinal fluid (CSF) [167].

##### 3.2.3. High-level preprocessing steps

High-level techniques for pre-processing brain data are important, and using them accompanying preliminary pre-processing methods can enhance the accuracy of ASD recognition. These methods are applied after the standard pre-processing of functional and structural brain data. These include sliding window (SW) [48], data augmentation (DA) [83], functional connectivity matrix (FCM) estimation [107,108] and applying fast Fourier transformation (FFT) [93]. Furthermore, some of the researches utilized feature extraction [121] techniques and some also use feature selection methods. Precise information on reviewed studies is indicated in detail in Table 1.

##### 3.3. Deep neural networks

DL in various medical applications, including the diagnosis of ASD has become extremely popular in recent years. In this section of the paper, the types of DL networks used in ASD detection are examined, which include CNN, RNN, AE, DBN, CNN-RNN, and CNN-AE models. Notably, CNN is the most common structure in reviewed research; this is arguably due to their structure being suitable for finding patterns in ASD datasets; more straightforward implementation, and more accessible transfer learning compared to other methods. Details of each ASD diagnosis study using neuroimaging modalities and DL models are shown in Table 1. It can be noted from this table that, the neuroimaging modalities used in the diagnosis of ASD include sMRI, DTI, rs-fMRI, T-fMRI, fNIRS, and EEG with their data in 1D, 2D, and 3D format. It can be observed that CNN models are used in most of the

**Table 1**

Summary of articles published using DL methods for neuroimaging-based ASD detection.

| Work  | Datasets                         | Neuroimaging Modalities              | Number of Cases                             | Pipeline and Atlas                                 | High level Preprocessing   | DNN Toolbox | DNN                     | Performance Criteria (%)                            |
|-------|----------------------------------|--------------------------------------|---|--|--|-------------|-------------------------|---|
| [48]  | Clinical                         | T-fMRI<br>Residual fMRI              | 82 ASD<br>48 HC                             | MNI152   | SW   | –           | 2CC3D + MV              | F1-Score = 89                                       |
| [81]  | Clinical                         | T-fMRI                               | 82 ASD<br>48 HC                             | AAL  | SVE, C-SVE, H-SVE, Monte Carlo Approximation   | –           | 2CC3D + Sigmoid         | Acc = 97.32   |
| [82]  | HCP Dataset in the HAFNI Project | T-fMRI<br>rs-fMRI                    | 68 Subjects with 7 Tasks and 1 rs-fMRI Data | –  | Dictionary Learning and Sparse Coding  | –           | 3D-CNN + Softmax        | Acc = 94.61   |
| [83]  | Clinical                         | T-fMRI                               | 21 ASD<br>19 HC                             | AAL  | DA   | Keras       | LSTM + Sigmoid          | Acc = 69.8  |
| [84]  | Different Datasets               | T-fMRI<br>rs-fMRI<br>Phenotypic Info | 1711 ASD<br>15903 HC                        | AAL  | DWT and Different Techniques   | Keras       | 2D-CNN + Softmax        | AUC = 0.92<br>Acc = 85.19                           |
| [85]  | Clinical                         | T-fMRI                               | 82 ASD<br>48 HC                             | AAL  | SW<br>Corrupting Strategy  | –           | 2CC3D + Sigmoid         | Acc = 87.1  |
| [85]  | ABIDE-I                          | rs-fMRI                              | 41 ASD<br>54 HC                             | AAL  | Prediction Distribution Analysis   | –           | 2CC3D + Sigmoid         | Acc = 85.3  |
| [86]  | ABIDE-I                          | rs-fMRI                              | 379 ASD, 395 HC                             | CPAC + All ABIDE Atlases                           | FCM  | –           | 3D-CNN + Sigmoid        | Acc = 73.3  |
|       | ABIDE II                         |                                      | 163 ASD, 230 HC                             |  |  |             |                         |   |
| [87]  | ABIDE-I                          | rs-fMRI                              | 505 ASD<br>530 HC                           | CPAC + CC-200<br>CPAC + AAL<br>CPAC + Dosenbach160 | FCM, DA  | PyTorch     | AE + SLP                | Acc = 70.1<br>Sen = 67.8<br>Spec = 72.8             |
| [88]  | ABIDE-I                          | rs-fMRI                              | 872 Subjects                                | CPAC + HO  | –  | –           | G-CNNs + Softmax        | Acc = 70.86   |
| [89]  | ABIDE-I                          | rs-fMRI                              | 474 ASD<br>539 HC                           | CCS + AAL  | FCM  | –           | BrainNetCNN + Softmax   | Acc = 68.7<br>Sen = 69.2<br>Spe = 68.3              |
| [90]  | ABIDE-I                          | rs-fMRI                              | 13 ASD<br>22 HC                             | AAL  | Qcut, NMI Statistic Matrix   | –           | DAE                     | Acc = 54.49   |
| [91]  | ABIDE                            | rs-fMRI                              | 11 ASD<br>16 HC                             | –  | Convert NII Files to PNG Images  | Caffe       | LeNet-5                 | Acc = 100<br>Sen = 99.99<br>Spec = 100              |
| [92]  | ABIDE-I                          | rs-fMRI                              | 55 ASD<br>55 HC                             | NIAK + AAL   | FCM, Feature Selection   | –           | Multiple SAEs + Softmax | Acc = 86.36   |
| [93]  | ABIDE-I                          | rs-fMRI                              | 54 ASD<br>62 HC                             | –  | FFT  | Keras       | MCNNes + SR             | Acc = 72.73<br>Sen = 71.2<br>Spec = 73.48           |
|       | ABIDE-II<br>ABIDE-I + II         |                                      | 156 ASD<br>187 HC                           |  | Dimension Reduction  | Theano      |                         |   |
| [94]  | ABIDE                            | rs-fMRI                              | 542 ASD<br>625 HC                           | CPAC + All Atlases                                 | Creating Stochastic Parcellations by Poisson Disk Sampling                                     | –           | 3D-CNN + VM             | Acc = 72  |
| [95]  | ABIDE-I                          | rs-fMRI                              | 465 ASD<br>507 HC                           | DPARSF + AAL                                       | FCM  | Keras       | VAE                     | –   |
| [96]  | ABIDE-I                          | rs-fMRI                              | 539 ASD<br>573 HC                           | CCS + Craddock 200                                 | DA   | Keras       | LSTM + Sigmoid          | Acc = 68.5  |
| [97]  | ABIDE                            | rs-fMRI<br>Phenotypic Info           | 505 ASD<br>530 HC                           | CC200  | Slice timing, Spatial Standardization, Smoothing, Filtering, Removing Covariates, FCM, AE-MKFC | –           | SAE + Clustering        | Acc = 61<br>F1-Score = 60.2                         |
| [98]  | ABIDE                            | rs-fMRI                              | 42 ASD<br>42 HC                             | –  | Independent Components   | –           | SAE + Softmax           | Acc = 87.21<br>Sen = 89.49<br>Spec = 83.73          |
| [99]  | ABIDE-I                          | rs-fMRI                              | NY site<br>UM site<br>US site<br>UC site    | CCS + AAL  | DA   | Keras       | LSTM + Sigmoid          | Acc = 74.8  |
| [100] | ABIDE-I                          | rs-fMRI                              | 408 ASD<br>401 HC                           | CPAC + HO<br>CPAC + AAL<br>CPAC + CC200            | –  | Keras       | DANN + Sigmoid          | Acc = 73.2<br>Sen = 74.5<br>Spec = 71.7             |
| [101] | ABIDE                            | rs-fMRI                              | At Least 60 Subjects                        | CCS + AAL  | DTL-NN Framework: Offline Learning, Transfer Learning FCM                                      | –           | SSAE + Softmax          | Avg Acc = 67.1<br>Avg Sen = 65.7<br>Avg spec = 68.3 |
| [102] | ABIDE I + II                     | rs-fMRI                              | 993 ASD<br>1092 HC                          | AAL<br>Schaefer-100<br>HO<br>Schaefer-400          | –  | –           | 1D-CNN + Softmax        | Acc = 68  |
| [103] | ABIDE-I                          | rs-fMRI                              |   | All Pipelines                                      | Single Volume Image Generator  | Keras       |                         |   |

(continued on next page)

**Table 1 (continued)**

| Work  | Datasets            | Neuroimaging Modalities             | Number of Cases             | Pipeline and Atlas                             | High level Preprocessing   | DNN Toolbox               | DNN                                | Performance Criteria (%)                                 |
|-------|---------------------|-------------------------------------|-----------------------------|--|--|---------------------------|------------------------------------|--|
|       |                     |                                     | 529 ASD<br>573 HC           |  |  |                           | 4 Deep Ensemble Learning + Sigmoid | Acc = 87<br>F1-score = 86<br>Recall = 85.2<br>Pre = 86.8 |
| [104] | ABIDE-II            | rs-fMRI                             | 303 ASD<br>390 HC           | –  | –  | –                         | 1D-CAE                             | Acc = 65.3   |
| [105] | ABIDE               | rs-fMRI                             | 40 ASD<br>40 HC             | CCS  | Thresholding Based Segmentation  | –                         | AlexNet + Softmax                  | Acc = 82.61  |
| [106] | ABIDE               | rs-fMRI                             | Whole Dataset               | All Pipelines                                  | DA Using SMOTE and Graph Network Motifs, FCM   | –                         | ASDDiagNet + SLP                   | Acc = 82<br>Sen = 79.1<br>Spec = 83.3                    |
| [107] | ABIDE-I             | rs-fMRI                             | 12 ASD<br>14 HC             | CPAC + SCSC                                    | Time Series Extraction from Different Regions, Connectivity Matrix, SMOTE Algorithm                  | PyTorch                   | Auto-ASDNetwork + SVM              | Acc = 80<br>Sen = 73<br>Spec = 83                        |
| [108] | ABIDE-I             | rs-fMRI                             | 505 ASD<br>530 HC           | CPAC + CC400                                   | FCM  | –                         | 2D-CNN + MLP                       | Acc = 70.20<br>Sen = 77.00<br>Spec = 61.00               |
| [109] | ABIDE               | rs-fMRI                             | 505 ASD<br>530 HC           | –  | FCM  | –                         | 1D CNN-AE + Softmax                | Acc = 70<br>Sen = 74<br>Spec = 63                        |
| [110] | ABIDE-I             | rs-fMRI                             | 539 ASD<br>573 HC           | –  | –  | Theano                    | 3D-FCNN + Softmax                  | Mean DSC = 91.56   |
| [111] | ABIDE-I             | rs-fMRI                             | 501 ASD<br>553 HC           | DPARSF + AAL                                   | FCM, Converting to 1D-Vector   | –                         | SSAE + Softmax                     | Acc = 93.59<br>Sen = 92.52<br>Spec = 94.56               |
| [112] | ABIDE-I             | rs-fMRI                             | 100 ASD<br>100 HC           | –  | Online Dictionary Learning and Sparse Representation Techniques, Generating Spatial Overlap Patterns | Theano                    | 3D-CNN                             | Avg Acc = 70.5<br>Avg Sen = 74<br>Avg Spec = 67          |
| [113] | ABIDE-I             | rs-fMRI<br>Phenotypic Info          | 529 ASD<br>571 HC           | CPAC + HO                                      | Population Graph Construction, Feature Selection Strategies (RFE, PCA, AE)                           | Scikit-learn              | GCN + Softmax                      | Acc = 80.0   |
| [114] | ABIDE-I             | rs-fMRI<br>Phenotypic Info          | 403 ASD<br>468 HC           | CCS + CC200                                    | DA   | Keras                     | LSTM + Sigmoid                     | Acc = 70.1   |
| [115] | ABIDE-I             | rs-fMRI<br>s-MRI<br>Phenotypic Info | 505 ASD<br>530 HC           | CPAC + CC200                                   | FCM  | –                         | Two SDAE + MLP                     | Acc = 70<br>Sen = 74<br>Spec = 63                        |
| [116] | Clinical            | rs-fMRI<br>Fetal BOLD fMRI          | 75 Qualified Subjects       | –  | Extraction of Fetal Brain fMRI Data, SW  | PyTorch                   | 3D-CNN + Sigmoid                   | F1-score = 84<br>AUC = 91                                |
| [117] | ABIDE-I<br>ABIDE-II | rs-fMRI<br>s-MRI                    | 116 ASD<br>69 HC            | AAL  | Segmentation, Average Mean Time Series of Each ROI   | Theano                    | DBN + LR                           | Acc = 65.56<br>Sen = 84<br>Spec = 32.96                  |
| [118] | IMPAC               | rs-fMRI<br>s-MRI                    | 418 ASD<br>497 HC           | All Atlases                                    | FCM, Features Extraction from sMRI   | Keras<br>TensorFlow Caffe | Different Networks + VM            | AUC = 80   |
| [119] | ABIDE-I             | rs-fMRI<br>s-MRI                    | 368 ASD<br>449 HC           | CPAC + AAL<br>CPAC + CC200<br>CPAC + Destrieux | FCM, Fisher Score  | –                         | Ensemble of 5 Stacked AEs and MLP  | Acc = 85.06<br>Sen = 81<br>Spec = 89                     |
| [120] | NDAR                | rs-fMRI<br>s-MRI                    | 61 ASD<br>215 HC            | –  | Data-Driven Landmark Discovery Algorithm, Patch Extraction   | –                         | Multi-Channel CNN + Softmax        | Acc = 76.24  |
| [121] | NDAR                | All Modalities                      | 78 ASD<br>124 HC            | Proposed Atlas                                 | Probabilistic Independent Component Analysis (PICA), Extraction of PSD                               | –                         | SAEs + PSVM                        | Acc = 88.5<br>Sen = 85.1<br>Spec = 90.4                  |
| [122] | NDAR                | s-MRI                               | 60 ASD<br>211 HC            | –  | 3D Patches Extraction  | –                         | DDUNET                             | –  |
| [123] | ABIDE-I             | s-MRI                               | 21 ASD<br>21 HC             | –  | Segmentation, Shape Feature Extraction   | –                         | SNCAE + Softmax                    | Acc = 96.88  |
|       | NDAR/Pitt           |                                     | 16 ASD<br>16 HC             |  |  |                           |                                    |  |
|       | NDAR/IBIS           |                                     | 10 ASD<br>10 HC             |  |  |                           |                                    |  |
| [124] | ABIDE-I             | s-MRI                               | 78 ASD<br>104 HC            | Destrieux                                      | Construction of Individual Network, F-score  | –                         | SAE + Softmax                      | Acc = 90.39<br>Sen = 84.37<br>Spec = 95.88               |
| [125] | HCP<br>ABIDE-I      | s-MRI                               | 1113 HC<br>83 ASD<br>105 HC | Desikan–Killia                                 | Normalization, Apply One-Hot Coding  | TensorFlow Keras          | DEA                                | AUC = 63.9   |
| [126] | ABIDE<br>CombiRx    | s-MRI                               | 1112 Subjects               | –  | –  | Keras                     | DCNN + Sigmoid                     | Acc = 84<br>Sen = 77<br>Spec = 85                        |
| [127] | ABIDE-II            | s-MRI                               | –                           | DKT  | Segmentation   | PyTorch                   | FastSurfer CNN + Softmax           | –  |
| [128] | ABIDE-I             | s-MRI                               | 500 ASD<br>500 HC           |  | GABM Method, New Chromosome Encoding Scheme  | –                         | 3D-CNN + Softmax                   | Acc = 70   |

(continued on next page)

**Table 1 (continued)**

| Work  | Datasets           | Neuroimaging Modalities | Number of Cases    | Pipeline and Atlas                             | High level Preprocessing   | DNN Toolbox            | DNN                     | Performance Criteria (%)  |
|-------|--------------------|-------------------------|--------------------|--|--|------------------------|-------------------------|---|
| [129] | Clinical           | s-MRI                   | 48 HC              | –  | HO Cortical & Subcortical Structural Atlas   | Sparse Annotations, DA | Caffe                   | 3D-CNN + Softmax<br>Acc = 91.6<br>AUC = 94.1                      |
| [130] | ABIDE-I            | rs-fMRI                 | 270 ASD<br>305 HC  | CPAC + Brain-Netome Atlas (BNA)                | Filtering, Calculating Mean Time Series for ROIs Using BrainNetome Atlas (BNA), Normalization  | –                      | CNN-GRU + Sigmoid       | Acc = 74.54<br>Sen = 63.46<br>Spec = 84.33                        |
| [131] | Clinical           | fnIRS                   | 25 ASD<br>22 HC    | –  | Transformation of the Time Series to Three Variants  | Keras                  | 1D CNN-LSTM + Bagging   | Acc = 95.7<br>Sen = 97.1<br>Spec = 94.3                           |
| [132] | Clinical           | fnIRS                   | 25 ASD<br>22 HC    | –  | SW Converted into the 3D Tensor  | –                      | CGRNN                   | Acc = 92.2<br>Sen = 85.0<br>Spec = 99.4                           |
| [133] | Different Datasets | s-MRI                   | –                  | Various Methods                                | Geometric DA   | Theano                 | ConvNet                 | –   |
| [134] | ABIDE I + II       | rs-fMRI                 | 620 ASD<br>2085 HC | CPAC + HO                                      | Performed an Automatic Quality Control, Visually Inspection, Feature Extraction, Occlusion of Brain Regions                              | –                      | 3D-CNN + MV             | Acc = 64<br>F1-Score = 66   |
| [135] | ABIDE-I            | rs-fMRI Phenotypic Info | 184 ASD<br>110 HC  | CPAC   | Down Sampling  | –                      | 3D-CNN -LSTM + Softmax  | Acc = 77<br>F1-score = 78   |
| [136] | ABIDE-I            | rs-fMRI s-MRI           | 403 ASD<br>468 HC  | 264 ROIs Based Parcellation Scheme             | FCM, Different Features  | –                      | AE + DNN                | Acc = 79.2<br>AUC = 82.4  |
| [137] | ABIDE-I            | rs-fMRI                 | 505 ASD<br>530 HC  | CPAC + CC200                                   | FCM  | PyTorch                | CapsNet + K-Means       | Acc = 71<br>Sen = 73<br>Spec = 66                                 |
| [138] | ABIDE              | rs-fMRI                 | 184 ASD            | CCS  | Motion Realignment, Rigid Registration, Spatially Downsampled  | –                      | convGRU-CNN3D           | Acc = 67<br>F1-score = 71   |
| [139] | ABIDE              | rs-fMRI                 | 252 ASD<br>252 HC  | CPAC + CC200                                   | FCM, Multistage SAAK Transform, Feature Selection  | –                      | 1D-CNN + Softmax        | Acc = 74.55   |
| [140] | ABIDE              | rs-fMRI                 | 419 ASD<br>530 HC  | CPAC + CC200<br>CPAC + AAL<br>CPAC + Dosenbach | Multiple Functional Connectivity Based On 3 Atlases Using PCC  | –                      | SDA + different methods | Acc = 74.52<br>Sen = 80.69<br>Spe = 66.71<br>AUC = 80.26          |
| [141] | ABIDE-I            | rs-fMRI                 | 505 ASD<br>530 HC  | CPAC + AAL                                     | ROI Extraction   | PyTorch                | Parallel 3D & ResNet-18 | Acc = 74<br>Recall = 95<br>F1 score = 80.5                        |
| [142] | ABIDE              | MRI                     | 946 ASD<br>1046 HC | –  | Spatial Transformation   | –                      | Combination of DNNs     | Different Results   |
| [143] | ABIDE              | rs-fMRI                 | 79 ASD<br>105 HC   | DPARSF   | Low-Frequency Drifts, Nuisance Signal Removal  | –                      | RBM + SVM               | Acc = 83<br>Pre = 81<br>Recall = 81<br>F1-Score = 80.50           |
| [144] | ABIDE I ABIDE II   | rs-fMRI                 | 300 ASD<br>300 HC  | GCA<br>HO<br>DCA                               | Whole Brain Mask Preparation and ROIs Extraction, Partial and Full Correlation Methods Such As GLASSO, MDMC, PCCE, CRF Feature Reduction | TensorFlow             | 1D-CNN + Softmax        | Acc = 70.31<br>Sen = 67.66<br>Spe = 73<br>Pre = 71.55<br>AUC = 73 |
| [145] | IMPAC              | sMRI                    | 537 ASD<br>590 HC  | MSDL Functional Atlas                          | sMRI Measures of Cortical Thickness, Surface Area & Volume   | –                      | CNN + Softmax           | Acc = 69<br>Sen = 79<br>Spe = 68.9<br>AUC = 73.3                  |
|       |                    | rs-fMRI                 |                    |  | fMRI Connectomes, Dictionary Pair Learning   |                        |                         |   |
| [146] | ABIDE I            | MRI                     | 500 ASD<br>500 HC  | HO<br>SSA                                      | GABM   | –                      | 3D-CNN + Softmax        | Acc = 73  |
| [147] | ABIDE              | rs-fMRI                 | 525 ASD<br>532 HC  | CCS + Craddock 200                             | ROIs Extraction, Functional Connectivity Matrix, Graph Construction (k-NN Graph)   | Keras,<br>TensorFlow   | cGCN                    | Acc = 70.7  |
| [148] | ABIDE I            | sMRI                    | 518 ASD<br>567 HC  | SRI24  | Individual-Level Morphological Covariance Brain Networks   | –                      | 2D-CNN (ResNet)         | Acc = 71.8<br>Sen = 81.25<br>Spec = 68.75<br>F1-Score = 68.7      |
| [149] | ABIDE I            | rs-fMRI                 | 505 ASD<br>530 HC  | CPAC + CC200                                   | Functional Connectivity  | PyTorch                | ASD-SAENet              | Acc = 70.8<br>Sen = 62.2<br>Spec = 79.1                           |
| [150] | ABIDE I            | rs-fMRI                 | 40 Subjects        | MSDL   | Masking  | Keras,<br>TensorFlow   | 1D-CNN                  | Acc = 92<br>AUC = 97  |
| [151] | ABIDE I            | rs-fMRI                 |                    |  | MSTEPS   | –                      |                         |   |

(continued on next page)

**Table 1 (continued)**

| Work  | Datasets                                | Neuroimaging Modalities                   | Number of Cases               | Pipeline and Atlas                                  | High level Preprocessing   | DNN Toolbox       | DNN   | Performance Criteria (%)                                 |
|-------|---|---|-------------------------------|---|--|-------------------|---|--|
|       |   |   | 403 ASD<br>468 HC             | Bootstrap Analysis of Stable Clusters (BASC)<br>CCS |  |                   | Different CNN And RNN Networks Inception-ResNetV2 VGG-16, ResNet-50 | Acc = 74.74<br>Sen = 72.95<br>Spec = 76.28<br>Acc = 57.6 |
| [152] | ABIDE I                                 | rs-fMRI                                   | 74 ASD<br>98 HC               | —   | 2D Neuroimages Acquisition Stages<br>3D to the 2D Conversion                             | —                 | TensorFlow  | Inception-ResNetV2 Acc = 87                              |
| [153] | ABIDE I                                 | rs-fMRI                                   | 539 ASD<br>573 HC             | —   |  |                   |   |  |
|       | ABIDE II                                |   | 521 ASD<br>573 HC             |   |  |                   |   |  |
| [154] | ABIDE I                                 | rs-fMRI                                   | 402 ASD<br>464 HC             | CPAC, BASC, Power, CC200, AAL                       | ROIs Extraction, Functional Connectivity   | Keras, TensorFlow | DNN   | Acc = 88<br>Sen = 90<br>F1-score = 87<br>AUC = 96        |
| [155] | NDAR                                    | rs-fMRI, ADOS                             | 78 ASD<br>78 HC               | Different   | rs-fMRI Analysis and ROIs Extraction, PSD  | —                 | AE  | Acc = 93<br>Sen = 91<br>Spec = 94                        |
| [156] | 6 Different Databases                   | sMRI and fMRI in Task and Rest Conditions | 14178 Subjects                | AAL   | Functional Connectivity, GM Volume and Single-Participant Structural Similarity Matrices | —                 | 2D-CNN + Softmax  | Acc = 69.7062<br>AUROC = 72.98                           |
| [157] | King Abdulaziz University (KAU) Dataset | EEG                                       | 9 ASD<br>10 HC                | —   | Windowing, Filtering Process, RNN-GRU, FastICA   | Keras, TensorFlow | 2D-CNN + Softmax  | Acc = 99.5<br>Sen = 52.13<br>Spec = 96.21                |
| [158] | King Abdulaziz University (KAU) Dataset | EEG                                       | 12 ASD<br>4 HC                | —   | Re-Referencing, Filtering, Normalization, STFT   | —                 | 2D-CNN + Softmax  | Acc = 99.15<br>Sen = 99.19<br>Spec = 99.04               |
| [159] | Clinical                                | EEG                                       | 8 ASD<br>12 Epilepsy<br>18 HC | —   | Filtering, ICA, Segmentation, PSDED  | TensorFlow        | DCNN + Softmax  | Acc = 80   |
| [160] | Clinical                                | rs-EEG                                    | 86 ASD<br>89 HC               | —   | Segmentation, Filtering, DFT   | —                 | CNN with Q-Learning + Sigmoid                                       | Acc = 92.63  |

studies on automated autism detection using neuroimaging modalities. The high performance is achieved by the supervised learning tasks due to their well-known structures such as VGG and ResNet. Also, their intrinsic matching with the neuroimaging modalities format and interpretability make it easier for researchers to apply and debug them. These papers have contributed significantly in resolving difficulties due to CNNs and obtain higher performances of the various DL techniques used for ASD diagnosis are presented in the following sections.

### 3.3.1. Convolutional neural networks (CNNs)

In this section, the types of popular convolutional networks used in ASD diagnosis are surveyed. These networks involve 1D-CNN, 2DCNN, 3D-CNN models, and a variety of pre-trained networks such as VGG. In CNN models, feature extraction is unsupervised, which is an advantage. Also, increasing the convolutional layers help to extract high-level features. Besides the advantages of CNN models, they have many training parameters resulting in high computational load and the need for powerful computers to implement [168–171].

#### (1). 1D AND 2D-CNN

There are many spatial dependencies present in the data and it is difficult to extract these hidden signatures from the data. Convolution network uses a structure alike to convolution filters to extract these features properly and contribute to the knowledge that features should be processed taking into account spatial dependencies; so the number of network parameters are significantly reduced. The principal application of these networks is in image processing and due to the two-dimensional (2D) image inputs, convolution layers form 2D structures, which is why these networks are called 2D convolutional neural network (2D-CNN). By using another type of data, one-dimensional signals, the convolution layers' structure also resembles the data structure [172,173]. In convolution networks, assuming that various data sections do not

require learning different filters, the number of parameters are markedly lessened and make it feasible to train these networks with smaller databases [45]. Figure (6) shows the block diagram of 2D-CNN used for ASD detection.

#### (2). 3D-CNN

By transforming the data into three dimensions, the convolution network will also be altered to a three-dimensional format (Fig. 7). It should be noted that the manipulation of three-dimensional CNN (3D-CNN) networks are less beneficial than 1D-CNN and 2D-CNN networks for diverse reasons. First, the data required to train these networks must be much larger which conventionally such datasets are not utilizable and methods such as pre-training, which are extensively exploited in 2D networks, cannot be used here. Another reason is that with the more complicated structure of networks, it becomes much tougher to fix the number of layers, and network structure. The 3D activation map generated during the convolution of a 3D CNN is essential for analyzing data where volumetric or temporal context is crucial. This ability to analyze a series of frames or images in context has led to the use of 3D CNNs as tools for action detection and evaluation of medical imaging [174].

### 3.3.2. Deep belief networks (DBNs)

DBNs are not popular today as they used to be, and have been substituted by new models to perform various applications (e.g., autoencoders for unsupervised learning, generative adversarial networks (GAN) for generative modes [175], variational autoencoders (VAE) [176]). However, disregarding the restricted use of these networks in this era, their influence on the advancement of neural networks cannot be overlooked. The use of these networks in this paper is related to the feature extraction without a supervisor or pre-training of networks. These networks serve as unsupervised, consisting of several

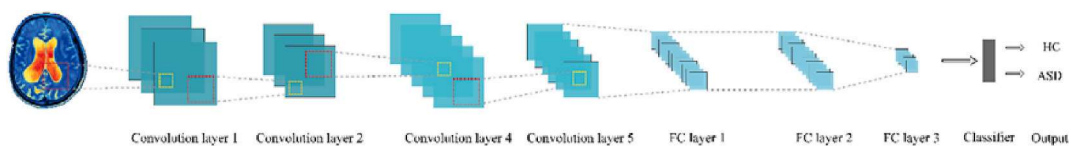


Fig. 6. Overall block diagram of a 2D-CNN used for ASD detection.

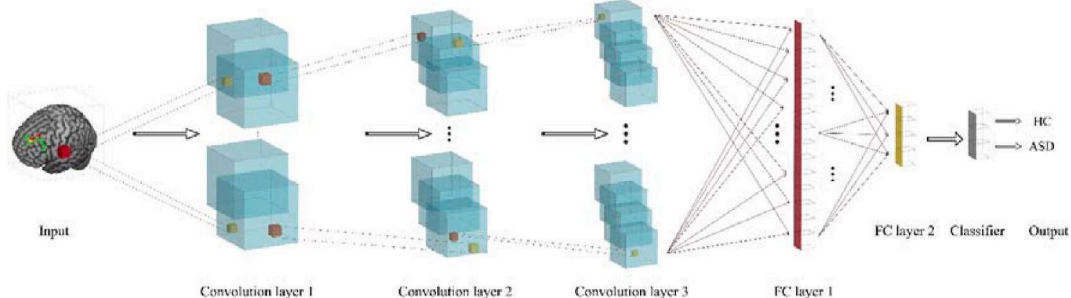


Fig. 7. Overall block diagram of a 3D-CNN used for ASD detection.

layers after the input layer, which are shown in [Figure \(8\)](#). The training of these networks is done greedily and from bottom to top, in other words, each separate layer is trained and then the next layer is appended. After training, these networks are used as a feature extractor, or the network weights are used as initial weights of a network for classification [45]. Training the DBN models is simpler than other DL models with improper performance and small number of data. One disadvantage of DBN models is that they do not consider the 2D structure of the input image. Thus, using them for machine vision applications is challenging [168–171].

### 3.3.3. Autoencoders (AEs)

Autoencoders (AEs) are more than 30 years old, and have undergone dramatic changes over the years to enhance their performance. But the overall structure of these networks has remained the same [45]. These networks consist of two parts: coder and decoder so that the first part of the input leads to coding in the latent space and the decoder part endeavors to convert the code into preliminary data ([Fig. 9](#)). Autoencoders are a special type of feedforward neural networks where the input is the same as the output. They compress the input into a lower-dimensional code and then reconstruct the output from this representation. The code is a compact “summary” or “compression” of the input, also called the latent-space representation. Various methods have been proposed to block the data memorization by the network, including sparse AE (SpAE) and denoising AE (DAE) [45]. Trained properly, the coder part of an Autoencoder can be used to extract features; creating an unsupervised feature extractor. The AE models are based on unsupervised training, which is an advantage. Also, these models suffer from disappearing gradients, which is a disadvantage [168–171].

### 3.3.4. Recurrent neural networks (RNNs)

In convolution networks, a kind of spatial dependencies in the data is addressed. But interdependencies between data are not confined to this model. For example, in time-series, dependencies may be highly distant from each other, on the other hand, the long-term and variable length of these sequences results in that the ordinary networks do not perform well enough to process these data. To overcome these problems, RNNs can be used. Long short-term memory (LSTM) structures are proposed to extract long term and short-term dependencies in the data ([Fig. 10](#)). Another well-known structure called gated recurrent unit (GRU) is developed after LSTM, and since then, most efforts have been made to enhance these two structures and make them resistant to challenges (e.g., GRU-D [177] is used to find the lost data). The RNN models have memory, and they can be used for disease prediction applications, which is an important advantage. The RNN models also suffer from disappearing gradients. It takes time to train these models due to their recurrent nature [168–171].

### 3.3.5. CNN-RNN

The initial idea in these networks is to utilize convolution layers to amend the performance of RNNs so that the advantages of both networks can be used; CNN-RNN, on the one hand, can find temporal dependencies with the aid of RNN, and on the other hand, it can discover spatial dependencies in data with the help of convolution layers [178]. These networks are highly beneficial for analyzing time series with more than one dimension (such as video) [179] but further to the simpler matter, these networks also yield the analysis of three-dimensional data so that instead of a more complex design of a 3D-CNN, a 2D-CNN with an RNN is occasionally used. The superiority of this model is due to the feasibility of employing pre-trained models. [Figure \(11\)](#) demonstrates

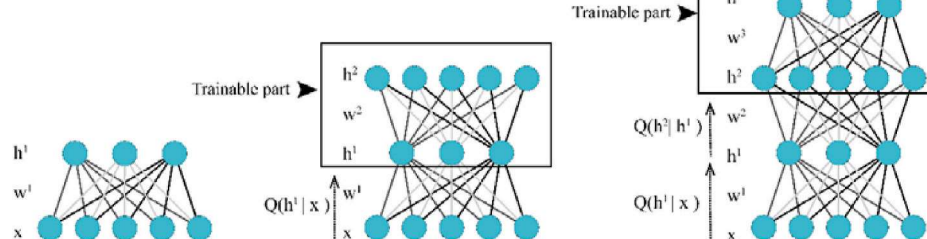
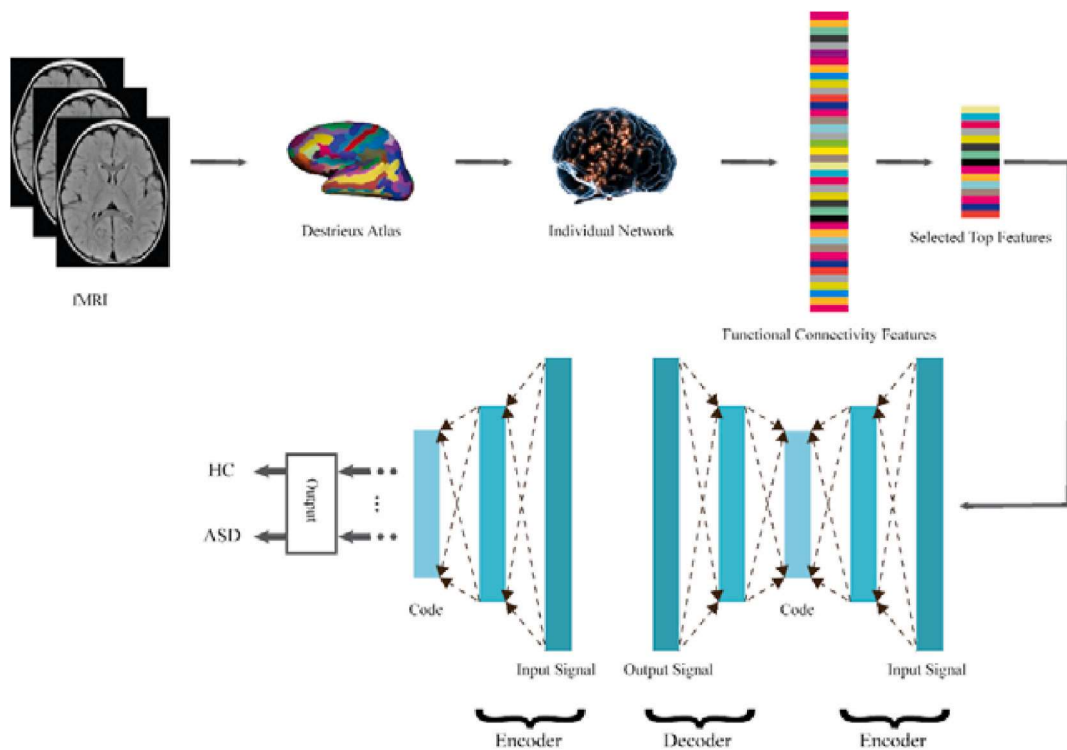
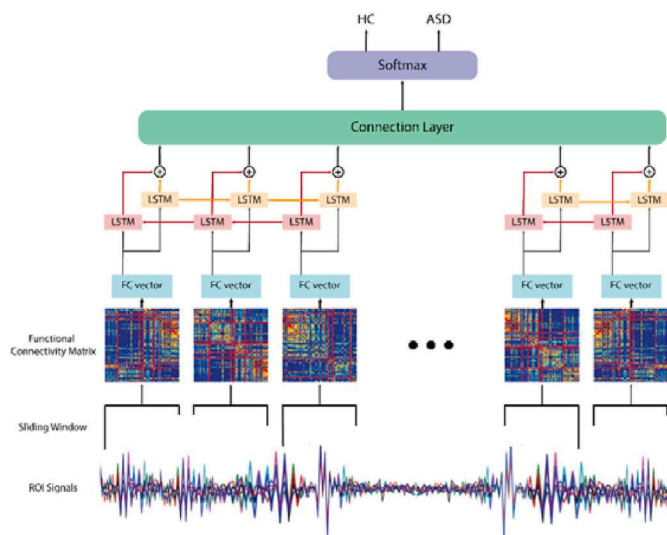


Fig. 8. Overall block diagram of a DBN used for ASD detection.



**Fig. 9.** Overall block diagram of an AE used for ASD detection.



**Fig. 10.** Overall block diagram of an LSTM used for ASD detection.

the CNN-RNN model. These models employ the advantages of CNN and RNN models in extracting features from medical data with high performance. Also, complicated training is the disadvantage of CNN-RNN models [168–171].

### 3.3.6. CNN-AE

In the construction of these networks, the principal aim and prerequisite have been to decrease the number of parameters. As shown before, changing merely the network layers to convolution markedly lessens the number of parameters; combining AE with convolution structures also makes a significant contribution. This helps to exploit higher dimensional data and extracts more information from the data without changing the size of the database. Similar structures, with or

without some modifications, are widely deployed for image segmentation [180], and likewise the unsupervised network can be applied for network pre-training or feature extraction. Figure (12) depicts the CNN-AE network used for ASD detection. The CNN-AE models perform well in extracting features from medical data due to convolution-based feature extraction using AE layers. Complicated training is the disadvantage of CNN-AE model [168–171,181].

Tables (1) and (2), provide the summary of papers published on detection and rehabilitation of ASD patients using DL, respectively.

## 4. Deep learning techniques for ASD rehabilitation

Rehabilitation tools are employed in multiple fields of medicine and their main purpose is to help the patients to recover after the treatment. Various and multiple rehabilitation tools using DL algorithms have been presented. Rehabilitation tools are used to help ASD patients using mobile, computer applications, robotic devices, cloud systems, and eye tracking, which will be discussed below. Also, the summary of papers published on rehabilitation of ASD patients using DL algorithms are shown in Table 2.

### 4.1. Mobile and software applications

Facial expressions are a key mode of non-verbal communication in children with ASD and play a pivotal role in social interactions. The use of brain computer interface (BCI) systems provides insight into the user's inner-emotional state. Valles et al. [185] conducted research focused on mobile software design to assist children with ASD. They aimed to design a smart iOS app based on facial images according to Figure (13). In this way, people's faces at different angles and brightness are first photographed and are turned into various emoji so that the autistic child can express his/her feelings and emotions. In this group's investigation [185], Kaggle's (The Facial Expression Recognition 2013) and KDEF (Kaggle's FER2013 and Karolinska Directed Emotional Faces) databases were used to train the VGG-16. In addition, the LEAP system was adapted to train the model at the University of Texas. The research

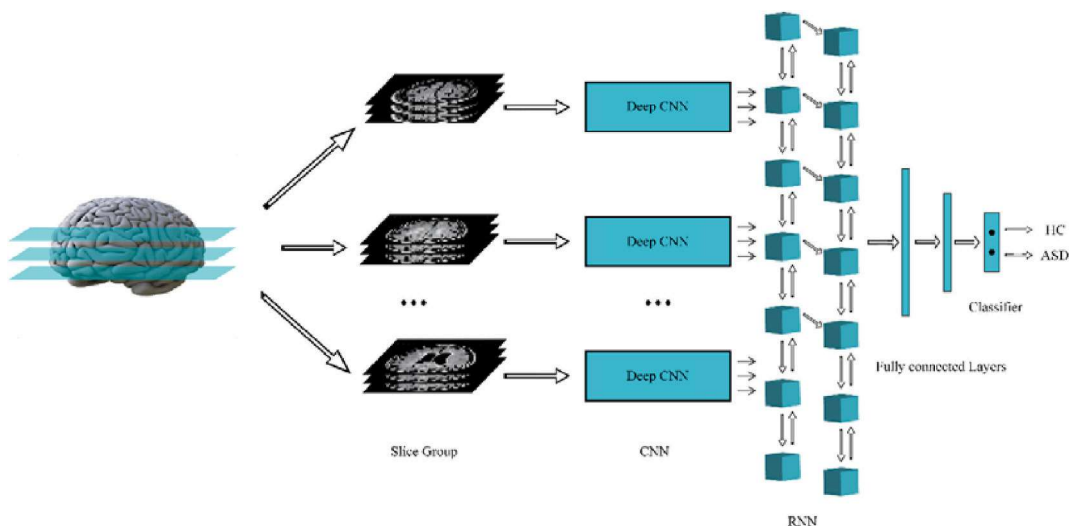


**Fig. 11.** Overall block diagram of a CNN-RNN used for ASD detection.

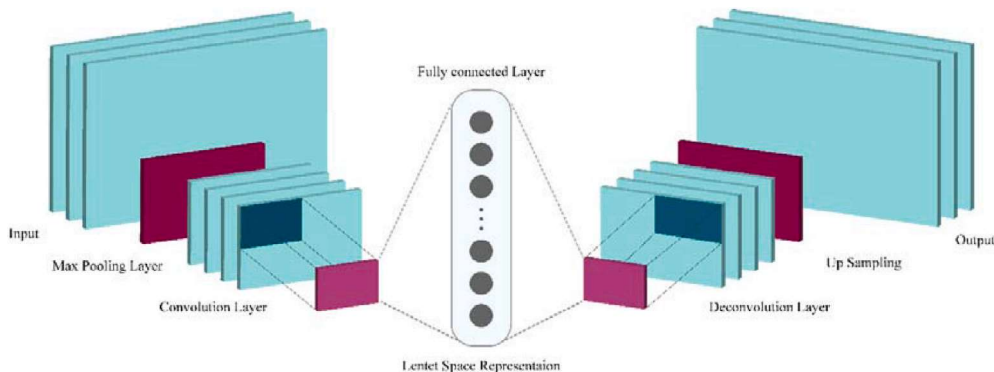


**Fig. 12.** Overall block diagram of a CNN-AE used for ASD detection.

provided the highest rate accuracy of 86.44%. In another similar study, they achieved an accuracy of 78.32% [183].

#### 4.2. Cloud systems

Mohammadian et al. [211] proposed a new application of DL to facilitate automatic stereotypical motor movement (SMM) identification by applying multi-axis inertial measurement units (IMUs). They applied CNN to transform multi-sensor time series into feature space. An LSTM network was then combined with CNN to obtain the temporal patterns for SMM identification. Finally, they employed the classifier selection voting approach to combine an ensemble of the best base learners. After various experiments, the superiority of their proposed procedure over other base methods was proven. Figure (14) shows the real-time SMM detection system. First, IMUs, which are wearable sensors, are used for data collection; the data can then be analyzed locally or remotely (using Wi-Fi to transfer data to tablets, cell phones, medical center servers, etc.) to identify SMMs. If abnormal movements are detected, an alarm will be sent to a therapist or parents.

#### 4.3. Eye tracking

Wu et al. [195] proposed a model of DL saliency prediction for autistic children. They used deep convolutional network (DCN) in their proposed paradigm, with a saliency map (SM) output. The fixation density map (FDM) was then processed by the single-side clipping (SSC) to optimize the proposed loss function as a true label along with the SM

saliency map. Finally, they exploited an ASD eye-tracking dataset to test the model. Their proposed model outperformed other base methods. Elbattah et al. [197] aimed to combine unsupervised clustering algorithms with DL to help ASD rehabilitation. The first step involved the visualization of the eye tracking path and the images captured from this step were fed to an AE to learn the features. Using AE features, clustering models are developed using the K-Means algorithm. Their method performed better than other state-of the art techniques.

### 5. Challenges

In this section, the most important challenges of ASD diagnosis are introduced using neuroimaging modalities, including neuroimaging datasets, tDCS and TMS challenges. Finally, the software and hardware challenges are discussed. These challenges are briefly presented in the following subsections.

#### 5.1. Neuroimaging datasets

The most important challenges of neuroimaging datasets are the inaccessibility of MRI modalities and other huge neuroimaging datasets, datasets with hybrid modalities, and datasets of various ASD disorders. In the following, these challenges are studied.

##### 5.1.1. Unavailability of MRI neuroimaging modalities datasets

In the ABIDE dataset, the diffusion tensor imaging (DTI) modality has not been presented for large number of subjects. Thus, limited

**Table 2**

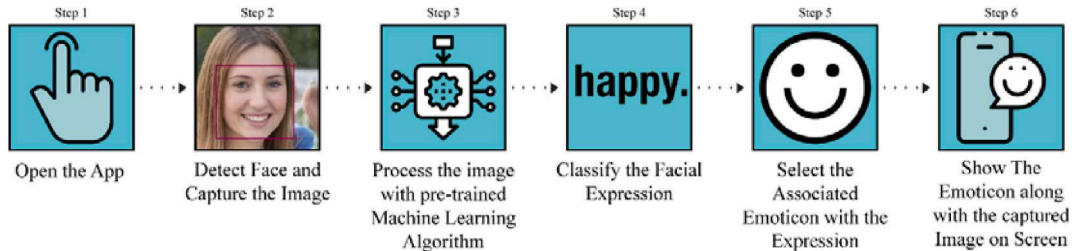
Summary of papers published on rehabilitation of ASD patients using DL algorithms.

| Work  | Datasets  | Type of Applications  | Number of Cases            | Preprocessing  | DNN Toolbox          | DNNs   | Performance Criteria (%)                        |
|-------|---|---|----------------------------|--|----------------------|--|---|
| [182] | OSIE  | –   | 20 ASD<br>19 HC            | HFM Construction, Filtering<br>Normalizing, DA   | Caffe<br>TensorFlow  | VGGNet +<br>Softmax                                    | Acc = 85<br>Sen = 80                            |
| [183] | KDEF  | Facial Expression Recognition   | 70 Individuals             | DA   | Keras                | DCNN +<br>Softmax                                      | Acc = 78.32                                     |
| [184] | Clinical  | Detecting Audio Regimes That Directly Estimate ASD Severity Social Affect scores  | 33 ASD                     | MFCC Spectrograms  | NA                   | Noisemes Network + RF<br>DiarTK<br>Diarization Network | Acc = 84.7                                      |
| [185] | Kaggle's FER2013                                | Facial Expression Recognition   | –                          | –  | Keras,<br>TensorFlow | DCNN +<br>Softmax                                      | Acc = 86.44                                     |
| [186] | SALICON   | ASD Classification  | 14 ASD<br>14 HC            | SalGAN Model, Feature Extraction   | –                    | SP-ASDNet  | Acc = 57.90<br>Rec = 59.21<br>Pre = 56.26       |
| [187] | BigFaceX  | Facial Expression Recognition   | 196 Subjects               | SW, Merge in the Channel Dimension, DA   | Keras                | TimeConvNet +<br>Softmax                               | Acc = 97.9                                      |
| [188] | Different Datasets                              | Suitable Courseware for Children with ASD   | –                          | Interactive and Intelligent Chat bot, NLP, Visual Aid  | –                    | Different Nets   | –   |
| [189] | Camera Images                                   | Estimating Visual Attention in Robot-Assisted Therapy                             | 6 ASD and ID               | Resizing, Frame Extraction, Visual Inspection Face Detection (Viola-Jones)   | –                    | R-CNN + KNN<br>MTCNN + Nave                            | Acc = 88.2<br>Pre = 83.3<br>Sen = 83.0          |
| [190] | Sensor Data                                     | Automatic SMM detection   | 6 ASD<br>5 HC              | Resampling, Filtering, SW  | Keras                | CNN-LSTM +<br>MV                                       | –   |
| [191] | KOMAA   | Facial Expression Recognition   | 55 subjects                | Segmentation, Different Features, Z Score  | –                    | CNN + SVM  | Acc = 96  |
| [192] | Story-Telling Narrative Corpora                 | ASD Classification  | 31 ASD<br>36 HC            | DA, ChineseWord2Vec  | –                    | LSTM   | Acc = 92  |
| [193] | Ext-Dataset (video dataset)                     | ASD Classification using Eye Tracking   | 136 ASD<br>136 HC          | TLD Method, Accumulative Histogram Computation   | Keras                | LSTM   | Acc = 92.6<br>Sen = 91.9<br>Spec = 93.4         |
| [194] | MIT1003   | Predicting Visual Attention of Children with ASD                                  | 300 Images                 | –  | –                    | DCN  | SIM = 67.8<br>CC = 76.9<br>AUC-J = 83.4         |
| [195] | Scan Path Data, Including Location and Duration | ASD Classification  | 14 ASD<br>14 HC            | DA Methods   | Pytorch              | ResNet18 +<br>Softmax                                  | Acc = 55.13<br>Sen = 63.5<br>Spec = 47.1        |
| [196] | UCI ML Repository                               | ASD Classification  | 704                        | Different Methods  | –                    | CNN  | Acc = 99.53<br>Sens = 99.39                     |
| [197] | Eye Tracking Scanpath                           | ASD Classification  | 29 ASD<br>30 HC            | Visualization of Eye-Tracking Scanpaths Scaling Down, PCA  | Keras, Sk-learn      | AE + K-Means   | Silhouette score = 60                           |
| [198] | Video Data                                      | Engagement Estimation of Children with ASD During a Robot-Assisted Autism Therapy | 30 children                | –  | Keras, TensorFlow    | CultureNet +<br>Softmax                                | ICC = 43.35<br>CCC = 43.18<br>PC = 45.17        |
| [199] | YouTube ASD Dataset                             | Modeling Typical and Atypical Behaviors in ASD Children                           | 68 video Clips             | Different Methods  | openCV, Caffe        | DCNN + DT  | Avg Pre = 73<br>Avg Recall = 75<br>Avg Acc = 71 |
| [200] | Video Dataset                                   | Behavioral Data Extracted from Video Analysis of Child-Robot Interactions.        | 5 ASD<br>7 HC              | Segmentation, Upper Body tracking, Laban Movement Analysis to Drive Weight, Different features                                     | –                    | CNN + Softmax  | Acc = 88.46<br>Pre = 89.12<br>Recall = 88.53    |
| [201] | Video Data                                      | Developing Automatic SMM Detection System   | 6 ASD                      | Resampling, Filtering, SW, Data Balancing, Normalizing   | Deepy Library        | CNN + SVM  | F1-score = 95                                   |
| [202] | ASD Screening                                   | Autism Screening  | 513 ASD<br>189 HC          | Cleaning Missing Values and Outliers, Visualization, Identity Mapping  | –                    | DENN +<br>Sigmoid                                      | Acc = 100<br>Sen = 100<br>F1-score = 99         |
| [203] | ASD Screening Datasets                          | Classification of Adults with ASD   | –                          | Handling of Missing Values, Variable Reduction, Normalization, and Label Encoding  | Keras                | DNN + Sigmoid  | Acc = 99.40<br>Sen = 97.89<br>Spec = 100        |
| [204] | GazeFollow4ASD Dataset                          | Gaze-Following  | 8 ASD<br>10 HC             | Saliency Map Generation (SMG)  | –                    | DNN + Softmax  | Acc = 79.94                                     |
| [205] | ADOS-2  | Child-Adult Speaker Classification  | 86 ASD<br>79 Others        | MFCC Feature Extraction  | –                    | GAN  | F1-Score = 78.27                                |
| [206] | Videos Dataset                                  | Gaze Direction Prediction   | 8 ASD<br>23 HC             | Gray-scaling, Face Detection By a Cascade Classifier With LBP Features, Eye Detection By Cascade Classifier With Haar Features, DA | Caffe                | 2D-CNN +<br>Softmax                                    | Acc = 97.38                                     |
| [207] | Image Dataset                                   | Face Image Classification   | 20 ASD<br>19 HC            | –  | –                    | ResNet-50 +<br>Softmax                                 | Acc = 89.2                                      |
| [208] | 72 ADOS Sessions                                | Estimate ADOS Scores  | 56 ASD<br>10 Other<br>6 HC | Segmentation, Feature Extraction, Sequential Forward Feature Selection (SFS)   | –                    | 1D-CNN   | RMSE = 4.65<br>Correlation = 0.72               |
| [209] | Clinical EEG                                    | –   | –                          | Filtering, Windowing   | Keras                | LSTM   | Acc = 93.27                                     |

(continued on next page)

**Table 2 (continued)**

| Work  | Datasets     | Type of Applications  | Number of Cases                | Preprocessing        | DNN Toolbox | DNNs | Performance Criteria (%) |
|-------|--------------|---|--------------------------------|----------------------|-------------|------|--------------------------|
| [210] | Clinical EEG | Anxiety Classification from EEG in Adolescents with Autism<br>EEG-Based Mental Stress Classification in Adolescents with Autism for Breathing Entrainment BCI | 8 ASD<br>5 HC<br>8 ASD<br>5 HC | Filtering, Windowing | Keras       | LSTM | Acc = 93.27              |

**Fig. 13.** Block diagram of iOS application for ASD rehabilitation.**Fig. 14.** Cloud system design for ASD rehabilitation.

studies have been done to diagnose ASD from DTI modalities and DL models. Another challenge is that neuroimaging modalities like diffusion weighted imaging (DWI) and perfusion-weighted imaging (PWI) have not been presented.

#### 5.1.2. Unavailability of other neuroimaging modalities datasets

As mentioned in the Introduction section, different functional neuroimaging modalities, including EEG [212], MEG [213], and fNIRS [214] are used for ASD diagnosis. The cost of EEG and fNIRS is lower than MRI modalities, but their efficiency in ASD diagnosis is high. Unfortunately, huge EEG and fNIRS datasets are not available freely for research. Also, to the best of our knowledge, no study has presented the ASD diagnosis using MEG modality and DL models due to the inaccessibility of MEG datasets.

#### 5.1.3. Unavailability of multimodality neuroimaging datasets

In clinical studies, multimodality techniques, including EEG-fNIRS [215], EEG-fMRI [216,217], EEG-MEG [218], and MEG-DTI [219], are being carried out for ASD diagnosis. Clinical studies have shown that using multimodality techniques play an efficient role in increasing the accuracy of ASD diagnosis [220]. Till now, multimodality neuroimaging datasets have not been available to the researchers, which is another challenge. The availability of such datasets can promote many studies in ASD diagnosis using various DL models.

#### 5.1.4. Unavailability of neuroimaging datasets with different types of ASDs

As mentioned before, ASD includes a wide range of disorders with varying levels [221]. But the purpose of most studies is to discriminate

ASD from healthy controls (HC). To the best of our knowledge, there is no study conducted to classify various types of ASD or its different levels due to the unavailability of datasets.

#### 5.2. Unavailability of TMS and tDCS for ASD

The Introduction section discussed brain stimulation using TMS and tDCS techniques. To use these methods, first, the brain is divided into different areas. Then, the brain area of interest is stimulated by a specialist [222,223]. An important challenge in using TMS and tDCS is that brain stimulation should be accurate; otherwise, the patient might encounter some side effects [224]. If the DL models are used along with TMS and tDCS techniques, the brain areas can be segmented with higher accuracy which promotes the brain stimulation with TMS and tDCS.

#### 5.3. Software and hardware challenges for ASD

This section presents the most important software and hardware challenges based on DL for ASD diagnosis. The sMRI modalities are recorded in 3D [225], and they are processed using 3D networks based on DL. Also, standard fMRI data is 4D [226] and requires 4D models based on DL for processing. In practice, using these networks is very challenging; as it requires huge memory, computational load, and hardware cost. Although 2D DL networks have been developed significantly, adding more layers and deepening the network imposes some constraints to the network. Including the number of layers, increasing the network parameters, makes training the network difficult and requires large number of training datasets which is difficult to obtain and

very expensive.

Another problem grappling the researchers is designing the DL-based rehabilitation systems with hardware resources. Nowadays, assistive tools such as Google Colab are available to researchers to improve the processing power. However, the problems still prevail when implementing these systems in real-world scenarios.

## 6. Discussion

In this study, we proposed a comprehensive overview of the investigations conducted in the scope of DL-based ASD diagnostic CAD systems as well as rehabilitation tools for ASD patients. In the field of ASD diagnosis, numerous papers have been published using functional and structural neuroimaging data as well as rehabilitation tools.

[Tables 1 and 2](#) respectively represent the details of ASD diagnosis and rehabilitation using DL models. In this section, the ML and DL techniques in ASD diagnosis are compared first. Afterwards, the other contents provided in [Table \(1\)](#) and [Table \(2\)](#) namely neuroimaging modalities, DL toolboxes, various DL models, and classification techniques are discussed.

### 6.1. Comparison of ML with DL methods for ASD diagnosis

Various studies have been proposed to diagnose ASD using ML techniques [227–237]. For example, Hyde et al. have reviewed applications of supervised machine learning methods for the diagnosis of ASD [227]. Song et al. have studied the classification and detection of ASD using ML methods and neuroimaging data [228]. Hosseinzadeh et al. [229] have reviewed ASD methods in the context of IoT devices systematically. Rahman et al. [230] have conducted a review on the analysis of ASD feature selection and classification. Pagnozzi et al. [231] have reviewed the studies on sMRI biomarkers in ASD detection using ML techniques. Xu et al. [232] have presented recent developments in identifying ASD using ML methods.

The preprocessing, feature extraction, feature selection (feature reduction), and classification are employed for ASD detection using ML techniques. Feature extraction is the most important section in ML models for ASD diagnosis. Choosing the appropriate feature extraction algorithms in CADS is very difficult, and, generally, it is done via trial and error, which is one of its important shortcomings [238–242]. Another shortcoming of ML technique is usage of large data that may lead to improper efficiency [243–246].

With the emergence of DL techniques, many scientists have employed these techniques for disease diagnosis [247–249]. The most important difference between ML and DL techniques is in feature extraction [168–171]. In the DL models, feature extraction and feature selection are carried out by deep layers [168–171]. Also, the efficiency of these models does not decrease by increasing the input neuroimaging data. To the best of our knowledge, this study is the first review paper discussing the ASD diagnosis using DL techniques which may help large number of young researchers to use the suitable AI method for the detection of ASD accurately.

### 6.2. Neuroimaging modalities for ASD diagnosis

[Table \(1\)](#) discuss the studies conducted on ASD diagnosis using neuroimaging modalities and DL models. In [Table \(1\)](#), sMRI, DTI, T-fMRI, rs-fMRI, and fNIRS modalities have been used to diagnose ASD. [Figure \(15\)](#) shows the number of papers published using various neuroimaging modalities for ASD diagnosis with DL technique.

It can be noted from [Figure \(15\)](#) that, rs-fMRI modality is used more than other methods for ASD diagnosis and rehabilitation.

### 6.3. DL toolboxes for ASD diagnosis and rehabilitation

A variety of DL toolboxes have been proposed for implementing deep

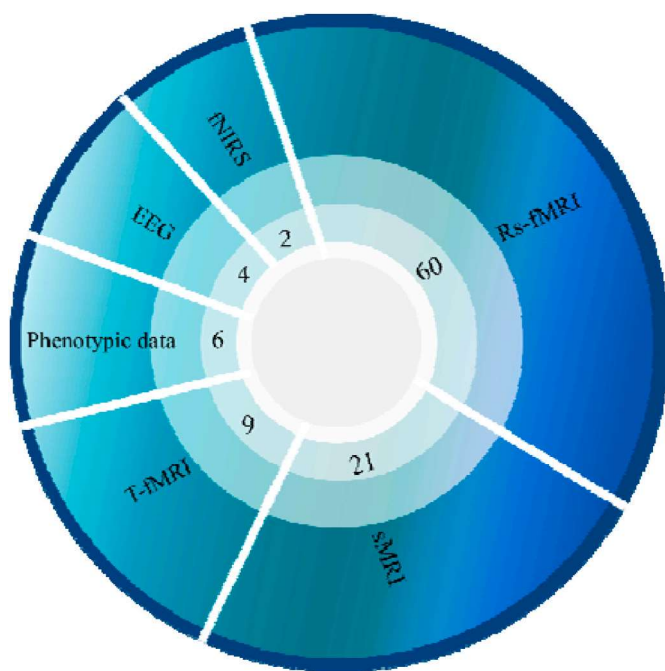


**Fig. 15.** Number of papers published using various modalities for ASD diagnosis with DL techniques.

networks. In [Tables 1 and 2](#) the types of DL toolboxes utilized for each study are depicted, and the total number of their usage is demonstrated in [Figure \(16\)](#).

The Keras toolbox is used in the majority of the studies due to its simplicity. Keras offers a consistent high-level application programming interface (APIs) to build the models more straightforward, and by using powerful backends such as TensorFlow, its performance is sound. Additionally, due to all pre-trained models and available codes on platforms such as GitHub, Keras is quite popular among researchers.

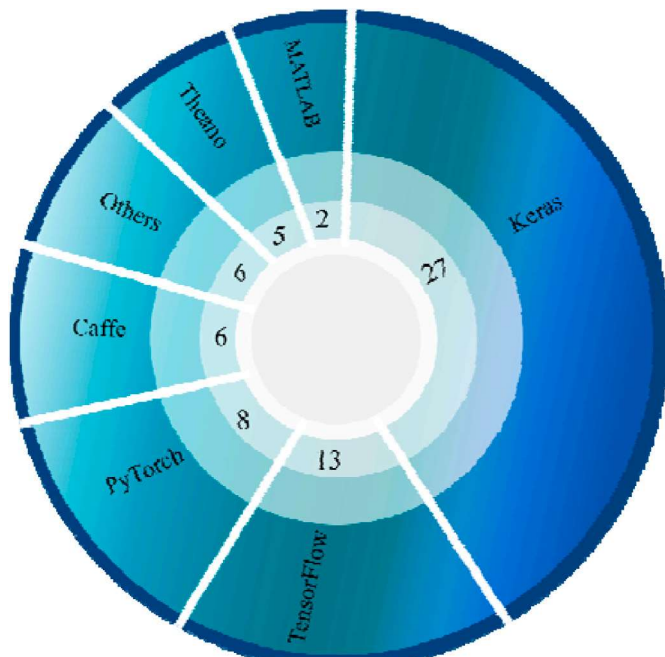


**Fig. 16.** Number of DL tools used for the diagnosis and rehabilitation of ASD patients in reviewed papers.

#### 6.4. DL methods for ASD diagnosis and rehabilitation

Various DL models have been presented in [Tables \(1\)](#) and [\(2\)](#) for ASD diagnosis and rehabilitation. [Tables \(1\)](#) and [\(2\)](#) show that CNN, RNN, AE, DBN, CNN-RNN, and CNN-AE models have been used for ASD diagnosis and rehabilitation. The number of DL networks used for the ASD detection in the reviewed works is shown in [Figure \(17\)](#).

Among the various DL architectures, CNN is found to be the most popular one as it has achieved more promising results compared to other deep methodologies. The AE, as well as RNN, has yielded favorable results. It can be noted that in recent years, the number of DL-based papers has increased exponentially due to their sound performance and also the availability of vast and thorough datasets.

#### 6.5. Classification methods for ASD diagnosis and rehabilitation

The number of various classification algorithms used in DL networks is shown in [Figure \(18\)](#). One of the best and most widely used is the Softmax algorithm ([Tables \(1\)](#) and [\(2\)](#)). It is most popular since it is differentiable in the entire domain and computationally less expensive.

### 7. Future works

In this section, future works on ASD diagnosis using neuroimaging modalities and DL models are presented. The future works include developing datasets, DL methods, and rehabilitation systems, which are discussed in the following sections.

#### 7.1. Future works in datasets

In Section 5 (Challenges), the available datasets were discussed. In this section, the future works regarding datasets, including presenting various structural and functional neuroimaging modalities, datasets of different types of ASD, and multimodality datasets are discussed.

##### 7.1.1. Future works in neuroimaging datasets

As mentioned before, the ABIDE dataset includes different MRI imaging modalities of ASD patients. In section 5, it was discussed that this

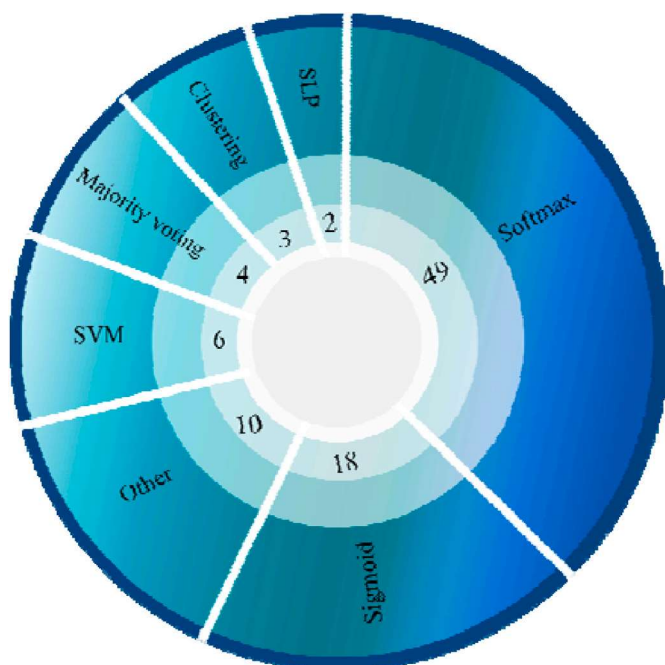


**Fig. 18.** Number of various classification algorithms used for the detection of ASD and rehabilitation in DL.

dataset consists of images of diffusion tensor imaging (DTI) modalities of few subjects and does not have images of diffusion weighted imaging (DWI) modality. Therefore, providing available datasets of DTI [34] and DWI [250] for ASD diagnosis using DL models in future studies is very important.

Also, a dataset [63,64] was provided for studies that include EEG signals of patients suffering from ASD and healthy controls (HC). This dataset has limited number of subjects. Therefore, DL studies have not focused on it. Also, there is no public dataset available on MEG and fNIRS modalities provided for the researchers. In future works, providing these datasets will help the researcher's to develop novel accurate ASD diagnosis systems using DL methods.

##### 7.1.2. Future works in neuroimaging datasets with different types of ASD

The ASD has various types and intensities [251]. As mentioned in the challenges section, there is no freely available neuroimaging dataset. In future studies, with more freely available datasets on ASD patients of different types and intensities can help to detect ASD accurately using DL models.

##### 7.1.3. Future works in multimodality neuroimaging datasets

In clinical research, EEG-fNIRS, EEG-fMRI, EEG-MEG, and MEG-DTI multi-modalities are used for ASD diagnosis [215–219]. Providing public datasets for these modalities can help the researchers to develop the DL models for ASD diagnosis.

### 7.2. Future works in deep learning methods for ASD diagnosis

In this paper, various DL methods were studied for ASD diagnosis using neuroimaging modalities. According to [Tables \(1\)](#) and [\(2\)](#), standard DL methods have been used for ASD diagnosis. In the following sections few suggestions are given for using DL methods which include attention techniques [252,253], adversarial techniques [254,255], and transformer techniques [256,257].

#### 7.2.1. Deep attention techniques

In recent years, attention techniques have become one of the most important concepts in DL [252–254,258]. These models are used in

**Fig. 17.** Number of DL networks used for ASD detection and rehabilitation in the reviewed works.

machine vision [259], speech processing [260], etc. The main idea of attention mechanism is that each time the model predicts the output, the parts of the input in which the most relevant information are concentrated, are processed instead of the whole sequence [261]. Some of these methods include deep attention-based RNNs [262], deep attention auto-encoders [263], deep attention CNN [264], and graph attention CNN [265]. Attention-based models provide a more accurate interpretation and a better description of information than basic models. In future studies, these models can be used for ASD diagnosis using neuroimaging modalities.

#### 7.2.2. Data augmentation techniques

The data shortage is a challenging problem for the scientists in disease diagnosis using DL techniques. Hence, various data augmentation techniques have been proposed [254,255]. GAN models are one of the most popular data augmentation techniques used to resolve the data shortage problems in ASD diagnosis using DL technique. Recently, the simple Copy-Paste methods have been presented for data augmentation [266]. In future studies, this method can also be used for data augmentation for ASD diagnosis using neuroimaging modalities.

#### 7.2.3. Transformer techniques

The transformer techniques are one of the most recent DL methods recently used for medical data classification [256,257]. The first work on transformer models has been introduced in [267]. In this architecture, the self-attention mechanism has been used along with the encoder and decoder [267]. In future studies, this model can be used for ASD diagnosis. Also, new transformer models like graph transformer networks [268] and deep diffeomorphic transformer networks [269] can be used in ASD diagnosis.

### 7.3. Future works in rehabilitation systems for ASD

Many researchers have proposed various DL-based rehabilitation tools to aid the ASD patients. Designing a reliable, accurate, and wearable low power consumption DL algorithm-based device is the future tool for ASD patients. An achievable rehabilitation tool is to wear smart glasses to help the children with ASD. These glasses with built-in cameras will acquire the images from the different directions of environment. Then the DL algorithm processes these images and produces meaningful images for the ASD children to better communicate with their surroundings.

Nowadays, cloud computing is one of the most important medical technologies, and various studies have been used it for disease diagnosis applications [269]. It helps to store data in the cloud space and implement various DL models [270]. In future studies, cloud computing can be used for ASD diagnosis using neuroimaging modalities and DL techniques.

Also, in future studies, the internet of things (IoT) can be used for ASD diagnosis. Lack of access to specialists in brain centers and hospitals is a challenge to diagnose ASD patients accurately. Hence we feel that,

### Appendix A. Statistical Metrics

This section demonstrates the equations for the calculation of each evaluation metric. In these equations, True positive (TP) is the correct classification of the positive class, True negative (TN) is the correct classification of the negative class, False positive (FP) is the incorrect prediction of the positives, False negative (FN) is the incorrect prediction of the negatives [168].

$$\text{Accuracy (Acc)} = \frac{TP + TN}{TP + TN + FP + FN} \quad (1)$$

$$\text{Specificity (Spec)} = \frac{TN}{TN + FP} \quad (2)$$

$$\text{Sensitivity (Sen)} = \frac{TP}{TP + FN} \quad (3)$$

$$\text{Precision (Prec)} = \frac{TP + TN}{TP + TN + FP + FN} \quad (4)$$

$$F1 - Score = 2 * \frac{\text{Prec} * \text{sens}}{\text{TPrec} + \text{Sens}} \quad (5)$$

#### Receiver Operating Characteristic Curve (ROC CURVE)

The receiver operating characteristic curve (ROC-curve) depicts the performance of the proposed model at all classification thresholds. It is the graph of true positive rate vs. false positive rate (TPR vs. FPR). Equations for calculation of TPR and FPR are presented below [168].

$$TPR = \frac{TP}{TP + TN} \quad (6)$$

$$FPR = \frac{FP}{FP + TN} \quad (7)$$

#### Area under the ROC Curve (AUC)

AUC presents the area under the ROC-curve from (0, 0) to (1, 1). It provides the aggregate measure of all possible classification thresholds. AUC has a range from 0 to 1. A 100% wrong classification will have AUC value of 0.0, while a 100% correct classified version will have the AUC value of 1.0. It has two folded advantages [168]. One is that it is scale invariant, which implies how well the model is predicted rather than checking the absolute values. The second advantage is that it is classification threshold-invariant as it will verify the performance of the model irrespective of the threshold being selected [168].

#### Appendix B

Tables (3) and (4) show all the abbreviations presented in this paper and their full forms, sorted alphabetically.

**TABLE 3**  
List of abbreviations, A through O.

| A       |  |
|---------|--|
| AAL     | Automated Anatomical Labeling                                      |
| AEs     | Autoencoders   |
| AI      | Artificial Intelligence  |
| API     | Application Programming Interface                                  |
| ASD     | Autism Spectrum Disorder   |
| AS      | Asperger's Syndrome  |
| APA     | American Psychiatric Association                                   |
| ADOS-2  | Autism Diagnostic Observation Schedule 2nd Edition                 |
| ADI-R   | Autism Diagnostic Interview-Revised                                |
| B       |  |
| BCI     | Brain Computer Interface   |
| C       |  |
| CADS    | Computer-Aided Diagnosis Systems                                   |
| CC200   | Craddock 200   |
| CC400   | Craddock 400   |
| CCS     | Connectome Computation System                                      |
| CPAC    | Configurable Pipeline for the Analysis of Connectomes              |
| CRF     | Conditional Random Forest  |
| CSF     | Cerebrospinal Fluid  |
| CDD     | Childhood Disintegrative Disorder                                  |
| CARS    | Childhood Autism Rating Scale                                      |
| D       |  |
| DA      | Data Augmentation  |
| DAE     | Denoising AE   |
| DBNs    | Deep Belief Networks   |
| DCA     | Diedrichsen Cerebellar Atlas                                       |
| DCN     | Deep Convolutional Network   |
| DL      | Deep Learning  |
| DPARSF  | Data Processing Assistant for rs-fMRI                              |
| DTI-MRI | Diffusion Tensor Imaging MRI                                       |
| DTI     | Diffusion Tensor Imaging   |
| DWI     | Diffusion Weighted Imaging   |
| DSM-5   | Diagnostic and Statistical Manual of Mental Disorders, 5th Edition |
| DISCO   | Diagnostic Interview for Social and Communication Disorder         |
| 3di     | Developmental, Dimensional, and Diagnostic Interview               |
| E       |  |

(continued on next page)

**TABLE 3 (continued)**

| A       |   |
|---------|---|
| ECoG    | Electrocorticography                                      |
| EEG     | Electroencephalography                                    |
| EZ      | Eickhoff-Zilles   |
| F       |   |
| FCM     | Functional Connectivity Matrix                            |
| FFS     | Forward Feature Selection                                 |
| FFT     | Fast Fourier Transform                                    |
| fMRI    | Functional MRI  |
| fNIRS   | Functional Near-Infrared Spectroscopy                     |
| FSL     | FMRIB software libraries                                  |
| G       |   |
| GABM    | Genetic Algorithm Based Brain Masking                     |
| GAN     | Generative Adversarial Network                            |
| GCA     | Gordon's Cortical Atlas                                   |
| GLASSO  | Graphical Least Absolute Shrinkage and Selection Operator |
| GM      | Gray Matter   |
| GRU     | Gated Recurrent Unit                                      |
| GARS    | Gilliam Autism Rating Scale                               |
| GPUs    | Graphic Processor Units                                   |
| H       |   |
| HIPAA   | Health Insurance Portability and Accountability           |
| HO      | Harvard-Oxford  |
| HOG     | Histogram of Oriented Gradients                           |
| HC      | Healthy Control   |
| I       |   |
| IMUs    | Inertial Measurement Units                                |
| IoT     | Internet of Things  |
| K       |   |
| KLD     | Kullback-Leibler Divergence                               |
| KAU     | King Abdulaziz University                                 |
| L       |   |
| LBP     | Local Binary Pattern                                      |
| LSTM    | Long Short-Term Memory                                    |
| M       |   |
| MCNNES  | Mixture of CNN Experts                                    |
| MEG     | Magnetoencephalography                                    |
| MDMC    | Max-Det Matrix Completion                                 |
| MFCC    | Mel-Frequency Cepstral Coefficients                       |
| MKFC-AE | Multi-kernel Fuzzy Clustering based AE                    |
| ML      | Machine Learning  |
| MLP     | Multilayer Perceptron                                     |
| MRI     | Magnetic Resonance Imaging                                |
| M-CHAT  | Modified Checklist for Autism in Toddlers                 |
| N       |   |
| NDAR    | National Database for Autism Research                     |
| NIAK    | Neuroimaging Analysis Kit                                 |
| NLP     | Natural Language Processing                               |
| NIBS    | Noninvasive Brain Stimulation                             |
| O       |   |
| 1D-CAE  | One-Dimensional CNN Autoencoder                           |

**TABLE 4**  
List of abbreviations, P through Z

| P       |  |
|---------|--|
| PCA     | Principal Component Analysis                               |
| PCC     | Pearson Correlation Coefficient                            |
| PCP     | Preprocess Connectome Projects                             |
| PICA    | Probabilistic Independent Component Analysis               |
| PSVM    | Probabilistic SVM  |
| PDD-NOS | Pervasive Developmental Disorder – Not Otherwise Specified |
| PWI     | Perfusion-Weighted Imaging                                 |
| R       |  |
| RF      | Random Forest  |
| RFE     | Recursive Feature Elimination                              |
| RL      | Reinforcement Learning                                     |
| RNNs    | Recurrent Neural Networks                                  |
| rs-fMRI | Resting-State fMRI   |
| RS      | Rett Syndrome  |
| S       |  |
| SAE     | Stacked AE   |
| SdAE    | Stacked Denoising AE                                       |

(continued on next page)

**TABLE 4 (continued)**

| P      |   |
|--------|---|
| SLP    | Single Layer Perceptron                 |
| SMG    | Saliency Map Generation                 |
| SMM    | Stereotypical Motor Movements           |
| sMRI   | Structural MRI                          |
| SpAE   | Sparse AE                               |
| SR     | Softmax Regression                      |
| SSA    | Subcortical Structural Atlas            |
| SVM    | Support Vector Machine                  |
| SW     | Sliding Window                          |
| T      |   |
| T-fMRI | Task-Based fMRI                         |
| 3D-CNN | Three Dimensional CNN                   |
| 2D-CNN | Two Dimensional CNN                     |
| tDCS   | Transcranial Direct Current Stimulation |
| TMS    | Transcranial Magnetic Stimulation       |
| V      |   |
| VAE    | Variational Autoencoders                |
| VS     | Voting Strategy                         |
| W      |   |
| WM     | White Matter                            |

**References**

- [1] J. Kang, X. Han, J. Song, Z. Niu, X. Li, The identification of children with autism spectrum disorder by SVM approach on EEG and eye-tracking data, *Comput. Biol. Med.* 120 (2020) 103722.
- [2] B.S. Abrahams, D.H. Geschwind, Advances in autism genetics: on the threshold of a new neurobiology, *Nat. Rev. Genet.* 9 (5) (2008) 341–355.
- [3] E. Stevens, D.R. Dixon, M.N. Novack, D. Granpeesheh, T. Smith, E. Linstead, Identification and analysis of behavioral phenotypes in autism spectrum disorder via unsupervised machine learning, *Int. J. Med. Inf.* 129 (2019) 29–36.
- [4] M.J. Maenner, K.A. Shaw, J. Baio, Prevalence of autism spectrum disorder among children aged 8 years—autism and developmental disabilities monitoring network, 11 sites, United States, 2016, *MMWR Surveillance Summaries* 69 (4) (2020) 1.
- [5] S. Yazdani, A. Capuano, M. Ghaziuddin, C. Colombi, Exclusion criteria used in early behavioral intervention studies for young children with autism spectrum disorder, *Brain Sci.* 10 (2) (2020) 99.
- [6] C.Y. Andy, R.S. Masters, Improving motor skill acquisition through analogy in children with autism spectrum disorders, *Psychol. Sport Exerc.* 41 (2019) 63–69.
- [7] T. Attwood, Asperger's Syndrome. Tizard Learning Disability Review, 2006.
- [8] E.E.J. Smeets, K. Pelc, B. Dan, Rett syndrome, *Molecular syndromology* 2 (3–5) (2011) 113–127.
- [9] S.H. Charan, Childhood disintegrative disorder, *J. Pediatr. Neurosci.* 7 (1) (2012) 55.
- [10] E. Singer, Diagnosis: redefining autism, *Nature* 491 (7422) (2012) S12–S13.
- [11] K.E. Towbin, Pervasive developmental disorder not otherwise specified, 2005.
- [12] American Psychiatric Association, & American Psychiatric Association, Diagnostic and Statistical Manual of Mental Disorders: DSM-5, 2013. United States.
- [13] F.R. Volkmar, B. Reichow, Autism in DSM-5: progress and challenges, *Mol. Autism.* 4 (1) (2013) 1–6.
- [14] <https://ourworldindata.org/grapher/prevalence-of-autistic-spectrum>.
- [15] O. Le Meur, A. Nebout, M. Cherel, E. Etchamendy, From Asperger autism to Kanner syndromes, the difficult task to predict where ASD people look at, *IEEE Access* 8 (2020) 162132–162140.
- [16] Z. Warren, M.I. McPheeeters, N. Sathe, J.H. Foss-Feig, A. Glasser, J. Veenstra-VanderWeele, A systematic review of early intensive intervention for autism spectrum disorders, *Pediatrics* 127 (5) (2011) e1303–e1311.
- [17] A. Khaleghi, H. Zarafshan, S.R. Vand, M.R. Mohammadi, Effects of non-invasive neurostimulation on autism spectrum disorder: a systematic review, *Clinical Psychopharmacology and Neuroscience* 18 (4) (2020) 527.
- [18] S. García-González, J. Lugo-Marín, I. Setién-Ramos, L. Gisbert-Gustemps, G. Arteaga-Henríquez, E. Díez-Villoría, J.A. Ramos-Quiroga, Transcranial Direct Current Stimulation in Autism Spectrum Disorder: A Systematic Review and Meta-Analysis, *European Neuropsychopharmacology*, 2021.
- [19] L.M. Oberman, P.G. Enticott, M.F. Casanova, A. Rotemberg, A. Pascual-Leone, J.T. McCracken, TMS in ASD Consensus Group, Transcranial magnetic stimulation in autism spectrum disorder: challenges, promise, and roadmap for future research, *Autism Res.* 9 (2) (2016) 184–203.
- [20] F. Thabtah, D. Peebles, Early autism screening: a comprehensive review, *Int. J. Environ. Res. Publ. Health* 16 (18) (2019) 3502.
- [21] T.P. Dorlack, O.B. Myers, P.W. Kodituwakk, A comparative analysis of the ADOS-G and ADOS-2 algorithms: preliminary findings, *J. Autism Dev. Disord.* 48 (6) (2018) 2078–2089.
- [22] M. Rutter, A. Le Couteur, C. Lord, *Autism Diagnostic Interview-Revised*, 29, Western Psychological Services, Los Angeles, CA, 2003, p. 30, 2003.
- [23] E. Schopler, R.J. Reichler, B.R. Renner, *The Childhood Autism Rating Scale (CARS)*, WPS, Los Angeles, CA, USA, 2010.
- [24] L. Wing, S.R. Leekam, S.J. Libby, J. Gould, M. Larcombe, The diagnostic interview for social and communication disorders: background, inter-rater reliability and clinical use, *JCPP (J. Child Psychol. Psychiatry)* 43 (3) (2002) 307–325.
- [25] J.E. Gilliam, *GARS: Gilliam Autism Rating Scale*, 1995. Pro-ed.
- [26] D. Skuse, R. Warrington, D. Bishop, U. Chowdhury, J. Lau, W. Mandy, M. Place, The developmental, dimensional and diagnostic interview (3di): a novel computerized assessment for autism spectrum disorders, *J. Am. Acad. Child Adolesc. Psychiatr.* 43 (5) (2004) 548–558.
- [27] M. Dereu, Modified checklist for autism in toddlers (m-chat), *Encyclopedia of Autism Spectrum Disorders* (2021) 2938–2943.
- [28] S.L. Hyman, S.E. Levy, S.M. Myers, Identification, evaluation, and management of children with autism spectrum disorder, *Pediatrics* 145 (1) (2020).
- [29] S.B. Mukherjee, Identification, evaluation, and management of children with autism spectrum disorder: American academy of pediatrics 2020 clinical guidelines, *Indian Pediatr.* 57 (10) (2020) 959–962.
- [30] H. Brentani, C.S.D. Paula, D. Bordini, D. Rolim, F. Sato, J. Portolese, J. T. McCracken, Autism spectrum disorders: an overview on diagnosis and treatment, *Brazilian Journal of Psychiatry* 35 (2013) S62–S72.
- [31] S. Mostafa, L. Tang, F.X. Wu, Diagnosis of autism spectrum disorder based on eigenvalues of brain networks, *IEEE Access* 7 (2019) 128474–128486.
- [32] A. Kazeminejad, R.C. Sotero, Topological properties of resting-state fMRI functional networks improve machine learning-based autism classification, *Front. Neurosci.* 12 (2019) 1018.
- [33] O. Dekhil, M. Ali, R. Haweel, Y. Elnakib, M. Ghazal, H. Hajjdiab, A. El-Baz, A comprehensive framework for differentiating autism spectrum disorder from neurotypicals by fusing structural MRI and resting state functional MRI, in: *Seminars in Pediatric Neurology*, 34, WB Saunders, 2020, July, p. 100805.
- [34] B.G. Travers, N. Adluru, C. Ennis, D.P. Tromp, D. Destiche, S. Doran, A. L. Alexander, Diffusion tensor imaging in autism spectrum disorder: a review, *Autism Res.* 5 (5) (2012) 289–313.
- [35] J. Vichnev, J.K.E. Wei, S.L. Oh, N. Arunkumar, E.W. Abdulhay, E.J. Ciaccio, U. R. Acharya, Autism spectrum disorder diagnostic system using HOS bispectrum with EEG signals, *Int. J. Environ. Res. Publ. Health* 17 (3) (2020) 971.
- [36] D. Haputhanthri, G. Brihadiswaran, S. Gunathilaka, D. Meedeniya, S. Jayarathna, M. Jaime, C. Harshaw, Integration of facial thermography in EEG-based classification of ASD, *Int. J. Autom. Comput.* (2020) 1–18.
- [37] J. Kang, T. Zhou, J. Han, X. Li, EEG-based multi-feature fusion assessment for autism, *J. Clin. Neurosci.* 56 (2018) 101–107.
- [38] T. Sinha, M.V. Munot, R. Sreemathy, An efficient approach for detection of autism spectrum disorder using electroencephalography signal, *IETE J. Res.* (2019) 1–9.
- [39] M. Sadeghi, R. Khosrowabadi, F. Bakouie, H. Mahdavi, C. Eslahchi, H. Pouretedmad, Screening of autism based on task-free fmri using graph theoretical approach, *Psychiatr. Res. Neuroimaging* 263 (2017) 48–56.
- [40] A. Kazeminejad, R.C. Sotero, Topological properties of resting-state fMRI functional networks improve machine learning-based autism classification, *Front. Neurosci.* 12 (2019) 1018.
- [41] J.C. Siero, D. Hermes, H. Hoogduin, P.R. Luijten, N.F. Ramsey, N. Petridou, BOLD matches neuronal activity at the mm scale: a combined 7 T fMRI and ECoG study in human sensorimotor cortex, *Neuroimage* 101 (2014) 177–184.
- [42] L. Xu, Q. Hua, J. Yu, J. Li, Classification of autism spectrum disorder based on sample entropy of spontaneous functional near infra-red spectroscopy signal, *Clin. Neurophysiol.* 131 (6) (2020) 1365–1374.
- [43] R.G. Port, J.C. Edgar, M. Ku, L. Bloy, R. Murray, L. Blaskey, T.P. Roberts, Maturation of auditory neural processes in autism spectrum disorder—a longitudinal MEG study, *Neuroimage: Clinical* 11 (2016) 566–577.

- [44] R.C. Deo, Machine learning in medicine, *Circulation* 132 (20) (2015) 1920–1930.
- [45] I. Goodfellow, Y. Bengio, A. Courville, Y. Bengio, Deep Learning, 1, MIT press, Cambridge, 2016. No. 2.
- [46] J. Dolz, C. Desrosiers, L. Wang, J. Yuan, D. Shen, I.B. Ayed, Deep CNN ensembles and suggestive annotations for infant brain MRI segmentation, *Comput. Med. Imag. Graph.* 79 (2020) 101660.
- [47] N. Ghassemi, A. Shoeibi, M. Rouhani, Deep neural network with generative adversarial networks pre-training for brain tumor classification based on MR images, *Biomed. Signal Process Control* 57 (2020) 101678.
- [48] X. Li, N.C. Dvornek, X. Papademetris, J. Zhuang, L.H. Staib, P. Ventola, J.S. Duncan, April. 2-channel convolutional 3D deep neural network (2CC3D) for fMRI analysis: ASD classification and feature learning, in: 2018 IEEE 15th International Symposium on Biomedical Imaging (ISBI 2018), IEEE, 2018, pp. 1252–1255.
- [49] Q. Delanoy, C.H. Pham, C. Cazorla, C. Tor-Díez, G. Dollé, H. Meunier, F. Rousseau, SegSRGAN: super-resolution and segmentation using generative adversarial networks—application to neonatal brain MRI, *Comput. Biol. Med.* 120 (2020) 103755.
- [50] R. Reed, R.J. MarksII, Neural Smithing: Supervised Learning in Feedforward Artificial Neural Networks, Mit Press, 1999.
- [51] G.E. Hinton, T.J. Sejnowski (Eds.), Unsupervised Learning: Foundations of Neural Computation, MIT press, 1999.
- [52] M. Wiering, Van Martijn Otterlo. Reinforcement Learning, 2012.
- [53] J. Eldridge, A.E. Lane, M. Belkin, S. Dennis, Robust features for the automatic identification of autism spectrum disorder in children, *J. Neurodev. Disord.* 6 (1) (2014) 1–12.
- [54] S. Bhat, U.R. Acharya, H. Adeli, G.M. Bairy, A. Adeli, Autism: cause factors, early diagnosis and therapies, *Rev. Neurosci.* 25 (6) (2014) 841–850.
- [55] A. Dejman, A. Khadem, A. Khorrami, May). Exploring the disorders of brain effective connectivity network in ASD: a case study using EEG, transfer entropy, and graph theory, in: 2017 Iranian Conference on Electrical Engineering (ICEE), IEEE, 2017, pp. 8–13.
- [56] N. Ghassemi, A. Shoeibi, M. Rouhani, H. Hosseini-Nejad, Epileptic seizures detection in EEG signals using TQWT and ensemble learning, in: 2019 9th International Conference on Computer and Knowledge Engineering (ICCKE), IEEE, 2019, October, pp. 403–408.
- [57] S. Bhat, U.R. Acharya, H. Adeli, G.M. Bairy, A. Adeli, Automated diagnosis of autism: in search of a mathematical marker, *Rev. Neurosci.* 25 (6) (2014) 851–861.
- [58] F. Thabtah, Machine learning in autistic spectrum disorder behavioral research: a review and ways forward, *Inf. Health Soc. Care* 44 (3) (2019) 278–297.
- [59] D. Eman, A.W. Emanuel, Machine learning classifiers for autism spectrum disorder: a review, in: 2019 4th International Conference on Information Technology, Information Systems and Electrical Engineering (ICITISEE), IEEE, 2019, November, pp. 255–260.
- [60] Autism brain imaging data exchange i, 2016. [http://fcon\\_1000.projects.nitrc.org/g/indi/abide/abide\\_i.html](http://fcon_1000.projects.nitrc.org/g/indi/abide/abide_i.html).
- [61] Abide preprocessed, in: <http://preprocessed-connectomesproject.org/abide/>.
- [62] N. Payakachat, J.M. Tilford, W.J. Ungar, National Database for Autism Research (NDAR): big data opportunities for health services research and health technology assessment, *Pharmacoeconomics* 34 (2) (2016) 127–138.
- [63] <https://malhaddad.kar.edu.sa/Pages-BCI-Datasets.aspx>.
- [64] R. Djemal, K. AlSharabi, S. Ibrahim, A. Alsuwailem, EEG-based Computer Aided Diagnosis of Autism Spectrum Disorder Using Wavelet, Entropy, and ANN 2017, BioMed research international, 2017.
- [65] M. Jenkinson, C.F. Beckmann, T.E. Behrens, M.W. Woolrich, S.M. Smith, *Fsl. Neuroimage* 62 (2) (2012) 782–790.
- [66] V. Popescu, M. Battaglini, W.S. Hoogstrate, S.C. Verfaillie, I.C. Sluimer, R.A. van Schijndel, MAGNIS Study Group, Optimizing parameter choice for FSL-Brain Extraction Tool (BET) on 3D T1 images in multiple sclerosis, *Neuroimage* 61 (4) (2012) 1484–1494.
- [67] B. Fischl, FreeSurfer. *Neuroimage* 62 (2) (2012) 774–781.
- [68] J. Ashburner, Computational anatomy with the SPM software, *Magn. Reson. Imag.* 27 (8) (2009) 1163–1174.
- [69] H.A. Jaber, H.K. Aljobouri, İ. Çankaya, O.M. Koçak, O. Algin, Preparing fMRI data for postprocessing: conversion modalities, preprocessing pipeline, and parametric and nonparametric approaches, *IEEE Access* 7 (2019) 122864–122877.
- [70] M. Behrooz, M.R. Daliri, H. Boyaci, Statistical analysis methods for the fMRI data, *Basic Clin. Neurosci.* 2 (4) (2011) 67–74.
- [71] B.Y. Park, K. Byeon, H. Park, FuNP (fusion of neuroimaging preprocessing) pipelines: a fully automated preprocessing software for functional magnetic resonance imaging, *Front. Neuroinf.* 13 (2019) 5.
- [72] J.A. Maldjian, P.J. Laurienti, R.A. Kraft, J.H. Burdette, An automated method for neuroanatomic and cytoarchitectonic atlas-based interrogation of fMRI data sets, *Neuroimage* 19 (3) (2003) 1233–1239.
- [73] N. Tzourio-Mazoyer, B. Landeau, D. Papathanassiou, F. Crivello, O. Etard, N. Delcroix, M. Joliot, Automated anatomical labeling of activations in SPM using a macroscopic anatomical parcellation of the MNI MRI single-subject brain, *Neuroimage* 15 (1) (2002) 273–289.
- [74] S.B. Eickhoff, K.E. Stephan, H. Mohlberg, C. Grefkes, G.R. Fink, K. Amunts, K. Zilles, A new SPM toolbox for combining probabilistic cytoarchitectonic maps and functional imaging data, *Neuroimage* 25 (4) (2005) 1325–1335.
- [75] R.S. Desikan, F. Ségonne, B. Fischl, B.T. Quinn, B.C. Dickerson, D. Blacker, R. J. Killiany, An automated labeling system for subdividing the human cerebral cortex on MRI scans into gyral based regions of interest, *Neuroimage* 31 (3) (2006) 968–980.
- [76] J. Talairach, Co-planar stereotaxic atlas of the human brain-3-dimensional proportional system, An approach to cerebral imaging (1988).
- [77] N.U. Dosenbach, B. Nardos, A.L. Cohen, D.A. Fair, J.D. Power, J.A. Church, B. L. Schlaggar, Prediction of individual brain maturity using fMRI, *Science* 329 (5997) (2010) 1358–1361.
- [78] R.C. Craddock, G.A. James, P.E. Holtzheimer III, X.P. Hu, H.S. Mayberg, A whole brain fMRI atlas generated via spatially constrained spectral clustering, *Hum. Brain Mapp.* 33 (8) (2012) 1914–1928.
- [79] M. Kunda, S. Zhou, G. Gong, H. Lu, Improving Multi-Site Autism Classification Based on Site-Dependence Minimization and Second-Order Functional Connectivity, *bioRxiv*, 2020.
- [80] <http://preprocessed-connectomes-project.org/abide/Pipelines.html>.
- [81] X. Li, N.C. Dvornek, Y. Zhou, J. Zhuang, P. Ventola, J.S. Duncan, Efficient interpretation of deep learning models using graph structure and cooperative game theory: application to asd biomarker discovery, in: International Conference on Information Processing in Medical Imaging, Springer, Cham, 2019, June, pp. 718–730.
- [82] Y. Zhao, Q. Dong, S. Zhang, W. Zhang, H. Chen, X. Jiang, T. Liu, Automatic recognition of fMRI-derived functional networks using 3-D convolutional neural networks, *IEEE (Inst. Electr. Electron. Eng.) Trans. Biomed. Eng.* 65 (9) (2017) 1975–1984.
- [83] N.C. Dvornek, D. Yang, P. Ventola, J.S. Duncan, Learning generalizable recurrent neural networks from small task-fMRI datasets, in: International Conference on Medical Image Computing and Computer-Assisted Intervention, Springer, Cham, 2018, September, pp. 329–337.
- [84] M. Leming, J.M. Görz, J. Suckling, Ensemble Deep Learning on Large, Mixed-Site fMRI Datasets in Autism and Other Tasks, 2020 arXiv preprint arXiv: 2002.07874.
- [85] X. Li, N.C. Dvornek, J. Zhuang, P. Ventola, J.S. Duncan, Brain biomarker interpretation in asd using deep learning and fMRI, in: International Conference on Medical Image Computing and Computer-Assisted Intervention, Springer, Cham, 2018, September, pp. 206–214.
- [86] M. Khosla, K. Jamison, A. Kuceyeski, M.R. Sabuncu, 3D convolutional neural networks for classification of functional connectomes, in: Deep Learning in Medical Image Analysis and Multimodal Learning for Clinical Decision Support, Springer, Cham, 2018, pp. 137–145.
- [87] T. Eslami, V. Mirjalili, A. Fong, A.R. Laird, F. Saeed, ASD-DiagNet: a hybrid learning approach for detection of autism spectrum disorder using fMRI data, *Front. Neuroinf.* 13 (2019) 70.
- [88] R. Anirudh, J.J. Thiagarajan, Bootstrapping graph convolutional neural networks for autism spectrum disorder classification, in: ICASSP 2019-2019 IEEE International Conference on Acoustics, Speech and Signal Processing (ICASSP), IEEE, 2019, May, pp. 3197–3201.
- [89] C.J. Brown, J. Kawahara, G. Hamarneh, Connectome priors in deep neural networks to predict autism, in: 2018 IEEE 15th International Symposium on Biomedical Imaging (ISBI 2018), IEEE, 2018, April, pp. 110–113.
- [90] D. Liao, H. Lu, March), Classify autism and control based on deep learning and community structure on resting-state fMRI, in: 2018 Tenth International Conference on Advanced Computational Intelligence (ICACI), IEEE, 2018, pp. 289–294.
- [91] X. Yang, S. Sarraf, N. Zhang, Deep learning-based framework for Autism functional MRI image classification, *Journal of the Arkansas Academy of Science* 72 (1) (2018) 47–52.
- [92] X. Guo, K.C. Dominick, A.A. Mina, H. Li, C.A. Erickson, L.J. Lu, Diagnosing autism spectrum disorder from brain resting-state functional connectivity patterns using a deep neural network with a novel feature selection method, *Front. Neurosci.* 11 (2017) 460.
- [93] M.A. Aghdam, A. Sharifi, M.M. Pedram, Diagnosis of autism spectrum disorders in young children based on resting-state functional magnetic resonance imaging data using convolutional neural networks, *J. Digit. Imag.* 32 (6) (2019) 899–918.
- [94] M. Khosla, K. Jamison, A. Kuceyeski, M.R. Sabuncu, Ensemble learning with 3D convolutional neural networks for functional connectome-based prediction, *Neuroimage* 199 (2019) 651–662.
- [95] H. Choi, Functional Connectivity Patterns of Autism Spectrum Disorder Identified by Deep Feature Learning, 2017 arXiv preprint arXiv:1707.07932.
- [96] N.C. Dvornek, P. Ventola, K.A. Pelphrey, J.S. Duncan, Identifying autism from resting-state fMRI using long short-term memory networks, in: International Workshop on Machine Learning in Medical Imaging, Springer, Cham, 2017, September, pp. 362–370.
- [97] H. Lu, S. Liu, H. Wei, J. Tu, Multi-kernel fuzzy clustering based on auto-encoder for fMRI functional network, *Expert Syst. Appl.* 159 (2020) 113513.
- [98] Z. Xiao, C. Wang, N. Jia, J. Wu, SAE-based classification of school-aged children with autism spectrum disorders using functional magnetic resonance imaging, *Multimed. Tools. Appl.* 77 (17) (2018) 22809–22820.
- [99] N.C. Dvornek, X. Li, J. Zhuang, J.S. Duncan, Jointly discriminative and generative recurrent neural networks for learning from fMRI, in: International Workshop on Machine Learning in Medical Imaging, Springer, Cham, 2019, October, pp. 382–390.
- [100] K. Niu, J. Guo, Y. Pan, X. Gao, X. Peng, N. Li, H. Li, Multichannel deep attention neural networks for the classification of autism spectrum disorder using neuroimaging and personal characteristic data, *Complexity* 2020 (2020).
- [101] H. Li, N.A. Parikh, L. He, A novel transfer learning approach to enhance deep neural network classification of brain functional connectomes, *Front. Neurosci.* 12 (2018) 491.
- [102] A. El Gazzar, L. Cerliani, G. van Wingen, R.M. Thomas, Simple 1-D convolutional networks for resting-state fMRI based classification in autism, in: 2019

- International Joint Conference on Neural Networks (IJCNN), IEEE, 2019, July, pp. 1–6.
- [103] M.R. Ahmed, Y. Zhang, Y. Liu, H. Liao, Single volume image generator and deep learning-based ASD classification, *IEEE Journal of Biomedical and Health Informatics* 24 (11) (2020) 3044–3054.
- [104] Y. Zhao, H. Dai, W. Zhang, F. Ge, T. Liu, Two-stage spatial temporal deep learning framework for functional brain network modeling, in: 2019 IEEE 16th International Symposium on Biomedical Imaging (ISBI 2019), IEEE, 2019, April, pp. 1576–1580.
- [105] B. Pugazhenthi, G.S. Senapathy, M. Pavithra, Identification of autism in MR brain images using deep learning networks, in: 2019 International Conference on Smart Structures and Systems (ICSSS), IEEE, 2019, March, pp. 1–7.
- [106] T. Eslami, J.S. Raiker, F. Saeed, Explainable and Scalable Machine-Learning Algorithms for Detection of Autism Spectrum Disorder Using fMRI Data, 2020 arXiv preprint arXiv:2003.01541.
- [107] T. Eslami, F. Saeed, Auto-ASD-network: a technique based on deep learning and support vector machines for diagnosing autism spectrum disorder using fMRI data, in: Proceedings of the 10th ACM International Conference on Bioinformatics, Computational Biology and Health Informatics, 2019, September, pp. 646–651.
- [108] Z. Sherkatghanad, M. Akhondzadeh, S. Salari, M. Zomorodi-Moghadam, M. Abdar, U.R. Acharya, V. Salari, Automated detection of autism spectrum disorder using a convolutional neural network, *Front. Neurosci.* 13 (2020) 1325.
- [109] K. Sairam, J. Naren, G. Vithya, S. Srivathsan, Computer aided system for autism spectrum disorder using deep learning methods, *Int. J. Psychosoc. Rehabil.* 23 (2019), 01.
- [110] J. Dolz, C. Desrosiers, I.B. Ayed, 3D fully convolutional networks for subcortical segmentation in MRI: a large-scale study, *Neuroimage* 170 (2018) 456–470.
- [111] C. Wang, Z. Xiao, B. Wang, J. Wu, Identification of autism based on SVM-RFE and stacked sparse auto-encoder, *IEEE Access* 7 (2019) 118030–118036.
- [112] Y. Zhao, F. Ge, S. Zhang, T. Liu, 3D deep convolutional neural network revealed the value of brain network overlap in differentiating autism spectrum disorder from healthy controls, in: International Conference on Medical Image Computing and Computer-Assisted Intervention, Springer, Cham, 2018, September, pp. 172–180.
- [113] S. Parisot, S.I. Ktena, E. Ferrante, M. Lee, R. Guerrero, B. Glocker, D. Rueckert, Disease prediction using graph convolutional networks: application to autism spectrum disorder and Alzheimer's disease, *Med. Image Anal.* 48 (2018) 117–130.
- [114] N.C. Dvornek, P. Ventola, J.S. Duncan, Combining phenotypic and resting-state fMRI data for autism classification with recurrent neural networks, in: 2018 IEEE 15th International Symposium on Biomedical Imaging (ISBI 2018), IEEE, 2018, April, pp. 725–728.
- [115] A.S. Heinsfeld, A.R. Franco, R.C. Craddock, A. Buchweitz, F. Meneguzzi, Identification of autism spectrum disorder using deep learning and the ABIDE dataset, *Neuroimage: Clinical* 17 (2018) 16–23.
- [116] X. Li, J. Hect, M. Thomason, D. Zhu, Interpreting age effects of human fetal brain from spontaneous fMRI using deep 3D convolutional neural networks, in: 2020 IEEE 17th International Symposium on Biomedical Imaging (ISBI), IEEE, 2020, April, pp. 1424–1427.
- [117] M.A. Aghdam, A. Sharifi, M.M. Pedram, Combination of rs-fMRI and sMRI data to discriminate autism spectrum disorders in young children using deep belief network, *J. Digit. Imag.* 31 (6) (2018) 895–903.
- [118] C. Mellena, A. Treacher, K. Nguyen, A. Montillo, Multiple deep learning architectures achieve superior performance diagnosing autism spectrum disorder using features previously extracted from structural and functional mri, in: 2019 IEEE 16th International Symposium on Biomedical Imaging (ISBI 2019), IEEE, 2019, April, pp. 1891–1895.
- [119] M. Rakić, M. Cabezas, K. Kushibar, A. Oliver, X. Lladó, Improving the detection of autism spectrum disorder by combining structural and functional MRI information, *Neuroimage: Clinical* 25 (2020) 102181.
- [120] G. Li, M. Liu, Q. Sun, D. Shen, L. Wang, Early diagnosis of autism disease by multi-channel CNNs, in: International Workshop on Machine Learning in Medical Imaging, Springer, Cham, 2018, September, pp. 303–309.
- [121] O. Dekhil, H. Hajjiab, A. Shalaby, M.T. Ali, B. Ayinde, A. Switala, A. El-Baz, Using resting state functional mri to build a personalized autism diagnosis system, *PLoS One* 13 (10) (2018), e0206351.
- [122] G. Li, M.H. Chen, G. Li, D. Wu, Q. Sun, D. Shen, L. Wang, A preliminary volumetric MRI study of amygdala and hippocampal subfields in autism during infancy, ISBI 2019, in: 2019 IEEE 16th International Symposium on Biomedical Imaging, IEEE, 2019, April, pp. 1052–1056.
- [123] M. Ismail, G. Barnes, M. Nitzen, A. Switala, A. Shalaby, E. Hosseini-Asl, A. El-Baz, A new deep-learning approach for early detection of shape variations in autism using structural mri, in: 2017 IEEE International Conference on Image Processing (ICIP), IEEE, 2017, September, pp. 1057–1061.
- [124] Y. Kong, J. Gao, Y. Xu, Y. Pan, J. Wang, J. Liu, Classification of autism spectrum disorder by combining brain connectivity and deep neural network classifier, *Neurocomputing* 324 (2019) 63–68.
- [125] W.H. Pinaya, A. Mechelli, J.R. Sato, Using deep autoencoders to identify abnormal brain structural patterns in neuropsychiatric disorders: a large-scale multi-sample study, *Hum. Brain Mapp.* 40 (3) (2019) 944–954.
- [126] S.J. Sujit, I. Coronado, A. Kamali, P.A. Narayana, R.E. Gabr, Automated image quality evaluation of structural brain MRI using an ensemble of deep learning networks, *J. Magn. Reson. Imag.* 50 (4) (2019) 1260–1267.
- [127] L. Henschel, S. Conjeti, S. Estrada, K. Diers, B. Fischl, M. Reuter, Fastsurfer-a fast and accurate deep learning based neuroimaging pipeline, *Neuroimage* 219 (2020) 117012.
- [128] H. Shahamat, M.S. Abadeh, Brain MRI analysis using a deep learning based evolutionary approach, *Neural Network* 126 (2020) 218–234.
- [129] J.E. Iglesias, G. Lerma-Usabiaga, L.C. Garcia-Peraza-Herrera, S. Martinez, P. M. Paz-Alonso, Retrospective head motion estimation in structural brain MRI with 3D CNNs, in: International Conference on Medical Image Computing and Computer-Assisted Intervention, Springer, Cham, 2017, September, pp. 314–322.
- [130] K. Byeon, J. Kwon, J. Hong, H. Park, Artificial neural network inspired by neuroimaging connectivity: application in autism spectrum disorder, in: 2020 IEEE International Conference on Big Data and Smart Computing (BigComp), IEEE, 2020, February, pp. 575–578.
- [131] L. Xu, Y. Liu, J. Yu, X. Li, X. Yu, H. Cheng, J. Li, Characterizing autism spectrum disorder by deep learning spontaneous brain activity from functional near-infrared spectroscopy, *J. Neurosci. Methods* 331 (2020) 108538.
- [132] L. Xu, X. Geng, X. He, J. Li, J. Yu, Prediction in autism by deep learning short-time spontaneous hemodynamic fluctuations, *Front. Neurosci.* 13 (2019) 1120.
- [133] B. Thyrreau, Y. Taki, Learning a cortical parcellation of the brain robust to the MRI segmentation with convolutional neural networks, *Med. Image Anal.* 61 (2020) 101639.
- [134] R.M. Thomas, S. Gallo, L. Cerliani, P. Zhutovsky, A. El-Gazzar, G. van Wingen, Classifying autism spectrum disorder using the temporal statistics of resting-state functional MRI data with 3D convolutional neural networks, *Front. Psychiatr.* 11 (2020) 440.
- [135] A. El-Gazzar, M. Quaak, L. Cerliani, P. Bloem, G. van Wingen, R.M. Thomas, A hybrid 3DCNN and 3DC-LSTM based model for 4D spatio-temporal fMRI data: an ABIDE autism classification study, in: OR 2.0 Context-Aware Operating Theaters and Machine Learning in Clinical Neuroimaging, Springer, Cham, 2019, pp. 95–102.
- [136] S. Mostafa, W. Yin, F.X. Wu, Autoencoder based methods for diagnosis of autism spectrum disorder, in: International Conference on Computational Advances in Bio and Medical Sciences, Springer, Cham, 2019, November, pp. 39–51.
- [137] Z. Jiao, H. Li, Y. Fan, Improving diagnosis of autism spectrum disorder and disentangling its heterogeneous functional connectivity patterns using capsule networks, in: 2020 IEEE 17th International Symposium on Biomedical Imaging (ISBI), IEEE, 2020, April, pp. 1331–1334.
- [138] M. Bengs, N. Gessert, A. Schlaefter, 4d Spatio-Temporal Deep Learning with 4d fMRI Data for Autism Spectrum Disorder Classification, 2020 arXiv preprint arXiv: 2004.10165.
- [139] Gupta, D., Vij, I., & Gupta, M. Autism Detection Using R-fMRI: Subspace Approximation and CNN Based Approach.
- [140] Y. Wang, J. Wang, F.X. Wu, R. Hayrat, J. Liu, AIMAFE: autism spectrum disorder identification with multi-atlas deep feature representation and ensemble learning, *J. Neurosci. Methods* (2020) 108840.
- [141] M. Tang, P. Kumar, H. Chen, A. Shrivastava, Deep multimodal learning for the diagnosis of autism spectrum disorder, *Journal of Imaging* 6 (6) (2020) 47.
- [142] F. Ke, S. Choi, Y.H. Kang, K.A. Cheon, S.W. Lee, Exploring the structural and strategic bases of autism spectrum disorders with deep learning, *IEEE Access* 8 (2020) 153341–153352.
- [143] M.R. Ahmed, M.S. Ahammed, S. Niu, Y. Zhang, Deep learning approached features for ASD classification using SVM, in: 2020 IEEE International Conference on Artificial Intelligence and Information Systems (ICAIIS), IEEE, 2020, March, pp. 287–290.
- [144] J.F.A. Ronicko, J. Thomas, P. Thangavel, V. Koneru, G. Langs, J. Dauwels, Diagnostic classification of autism using resting-state fMRI data improves with full correlation functional brain connectivity compared to partial correlation, *J. Neurosci. Methods* 345 (2020) 108884.
- [145] M. Zhang, X. Zhao, W. Zhang, A. Chaddad, A. Evans, J.B. Poline, Deep discriminative learning for autism spectrum disorder classification, in: International Conference on Database and Expert Systems Applications, Springer, Cham, 2020, September, pp. 435–443.
- [146] H. Shahamat, M.S. Abadeh, Brain MRI analysis using a deep learning based evolutionary approach, *Neural Network* 126 (2020) 218–234.
- [147] L. Wang, K. Li, X.P. Hu, Graph convolutional network for fMRI analysis based on connectivity neighborhood, *Network Neuroscience* 5 (1) (2021) 83–95.
- [148] J. Gao, M. Chen, Y. Li, Y. Gao, Y. Li, S. Cai, J. Wang, Multisite autism spectrum disorder classification using convolutional neural network classifier and individual morphological brain networks, *Front. Neurosci.* 14 (2021) 1473.
- [149] F. Almughim, F. Saeed, ASD-SAENet: a sparse autoencoder, and deep-neural network model for detecting autism spectrum disorder (ASD) using fMRI data, *Front. Comput. Neurosci.* 15 (2021) 27.
- [150] A. Mozhdefarabkhsh, S. Chitsazian, P. Chakrabarti, K.J. Rao, B. Kateb, M. Nami, A Convolutional Neural Network Model to Differentiate Attention Deficit Hyperactivity Disorder and Autism Spectrum Disorder Based on the Resting State fMRI Data, 2021.
- [151] M.A. Bayram, Ö.Z.E.R. İlyas, F. Temurtaş, Deep learning methods for autism spectrum disorder diagnosis based on fMRI images, *Sakarya University Journal of Computer and Information Sciences* 4 (1) (2021) 142–155.
- [152] N. Dominic, T.W. Cenggoro, A. Budiantoro, B. Pardamean, Transfer learning using inception-ResNet-v2 model to the augmented neuroimages data for autism spectrum disorder classification, *Commun. Math. Biol. Neurosci.* 2021 (2021). Article-ID.
- [153] R.N.S. Husna, A.R. Syafeeza, N.A. Hamid, Y.C. Wong, R.A. Raihan, Functional magnetic resonance imaging for autism spectrum disorder detection using deep learning, *Jurnal Teknologi* 83 (3) (2021) 45–52.
- [154] F.Z. Subah, K. Deb, P.K. Dhar, T. Koshiba, A deep learning approach to predict autism spectrum disorder using multisite resting-state fMRI, *Appl. Sci.* 11 (8) (2021) 3636.

- [155] O. Dekhil, M. Ali, A. Shalaby, A. Mahmoud, A. Switala, M. Ghazal, A. El-Baz, Identifying personalized autism related impairments using resting functional mri and ados reports, in: International Conference on Medical Image Computing and Computer-Assisted Intervention, Springer, Cham, 2018, September, pp. 240–248.
- [156] M.J. Leming, S. Baron-Cohen, J. Suckling, Single-participant structural similarity matrices lead to greater accuracy in classification of participants than function in autism in MRI, *Mol. Autism.* 12 (1) (2021) 1–15.
- [157] G. Bouallgue, R. Djemal, S.A. Alshebeili, H. Aldhalaan, A dynamic filtering DF-RNN deep-learning-based approach for EEG-based neurological disorders diagnosis, *IEEE Access* 8 (2020) 206992–207007.
- [158] M.N.A. Tawhid, S. Siuly, H. Wang, F. Whittaker, K. Wang, Y. Zhang, A spectrogram image based intelligent technique for automatic detection of autism spectrum disorder from EEG, *PLoS One* 16 (6) (2021), e0253094.
- [159] M. Ranjani, P. Suprja, March, Classifying the autism and epilepsy disorder based on EEG signal using deep convolutional neural network (DCNN), in: 2021 International Conference on Advance Computing and Innovative Technologies in Engineering (ICACITE), IEEE, 2021, pp. 880–886.
- [160] H. Dong, D. Chen, L. Zhang, H. Ke, X. Li, Subject sensitive EEG discrimination with fast reconstructable CNN driven by reinforcement learning: a case study of ASD evaluation, *Neurocomputing* 449 (2021) 136–145.
- [161] P. Bellec, C. Chu, F. Chouinard-Decorte, Y. Benhajali, D.S. Margulies, R. C. Craddock, The neuro bureau ADHD-200 preprocessed repository, *Neuroimage* 144 (2017) 275–286.
- [162] C. Yan, Y. Zang, DPARSF: a MATLAB toolbox for "pipeline" data analysis of resting-state fMRI, *Front. Syst. Neurosci.* 4 (2010) 13.
- [163] C. Craddock, S. Sikka, B. Cheung, R. Khanuja, S.S. Ghosh, C. Yan, M. Milham, Towards automated analysis of connectomes: the configurable pipeline for the analysis of connectomes (c-pac), *Front. Neuroinf.* 42 (2013) 10–3389.
- [164] T. Xu, Z. Yang, L. Jiang, X.X. Xing, X.N. Zuo, A connectome computation system for discovery science of brain, *Sci. Bull.* 60 (1) (2015) 86–95.
- [165] J.V. Manjón, MRI preprocessing, in: Imaging Biomarkers, Springer, Cham, 2017, pp. 53–63.
- [166] B.Y. Park, K. Byeon, H. Park, FuNP (fusion of neuroimaging preprocessing) pipelines: a fully automated preprocessing software for functional magnetic resonance imaging, *Front. Neuroinf.* 13 (2019) 5.
- [167] I. Despotović, B. Goossens, W. Philips, MRI segmentation of the human brain: challenges, methods, and applications, *Computational and mathematical methods in medicine* 2015 (2015).
- [168] A. Shoeibi, M. Khodatars, R. Alizadehsani, N. Ghassemi, M. Jafari, P. Moridian, P. Shi, Automated Detection and Forecasting of Covid-19 Using Deep Learning Techniques: A Review, 2020 arXiv preprint arXiv:2007.10785.
- [169] A. Shoeibi, M. Khodatars, N. Ghassemi, M. Jafari, P. Moridian, R. Alizadehsani, U. R. Acharya, Epileptic seizures detection using deep learning techniques: a review, *Int. J. Environ. Res. Publ. Health* 18 (11) (2021) 5780.
- [170] A. Shoeibi, M. Khodatars, M. Jafari, P. Moridian, M. Rezaei, R. Alizadehsani, U. R. Acharya, Applications of Deep Learning Techniques for Automated Multiple Sclerosis Detection Using Magnetic Resonance Imaging: A Review, 2021 arXiv preprint arXiv:2105.04881.
- [171] A. Shoeibi, N. Ghassemi, M. Khodatars, M. Jafari, P. Moridian, R. Alizadehsani, S. Nahavandi, Applications of Epileptic Seizures Detection in Neuroimaging Modalities Using Deep Learning Techniques: Methods, Challenges, and Future Works, 2021 arXiv preprint arXiv:2105.14278.
- [172] F. Chollet, Deep Learning mit Python und Keras: Das Praxis-Handbuch vom Entwickler der Keras-Bibliothek, MITP-Verlags GmbH & Co. KG, 2018.
- [173] A. Shoeibi, M. Khodatars, R. Alizadehsani, N. Ghassemi, M. Jafari, P. Moridian, D. Srinivasan, Automated Detection and Forecasting of Covid-19 Using Deep Learning Techniques: A Review, 2020 arXiv preprint arXiv:2007.10785.
- [174] L. Zou, J. Zheng, C. Miao, M.J. McKeown, Z.J. Wang, 3D CNN based automatic diagnosis of attention deficit hyperactivity disorder using functional and structural MRI, *IEEE Access* 5 (2017) 23626–23636.
- [175] A. Radford, L. Metz, S. Chintala, Unsupervised Representation Learning with Deep Convolutional Generative Adversarial Networks, 2015 arXiv preprint arXiv: 1511.06434.
- [176] C. Doersch, Tutorial on Variational Autoencoders, 2016 arXiv preprint arXiv: 1606.05908.
- [177] Z. Che, S. Purushotham, K. Cho, D. Sontag, Y. Liu, Recurrent neural networks for multivariate time series with missing values, *Sci. Rep.* 8 (1) (2018) 1–12.
- [178] J. Wang, Y. Yang, J. Mao, Z. Huang, C. Huang, W. Xu, Cnn-mn: a unified framework for multi-label image classification, in: Proceedings of the IEEE Conference on Computer Vision and Pattern Recognition, 2016, pp. 2285–2294.
- [179] Y. Fan, X. Lu, D. Li, Y. Liu, Video-based emotion recognition using CNN-RNN and C3D hybrid networks, in: Proceedings of the 18th ACM International Conference on Multimodal Interaction, 2016, October, pp. 445–450.
- [180] M. Chen, X. Shi, Y. Zhang, D. Wu, M. Guizani, Deep Features Learning for Medical Image Analysis with Convolutional Autoencoder Neural Network, *IEEE Transactions on Big Data*, 2017.
- [181] A. Shoeibi, N. Ghassemi, R. Alizadehsani, M. Rouhani, H. Hosseini-Nejad, A. Khosravi, S. Nahavandi, A comprehensive comparison of handcrafted features and convolutional autoencoders for epileptic seizures detection in EEG signals, *Expert Syst. Appl.* 163 (2021) 113788.
- [182] J. Xie, L. Wang, P. Webster, Y. Yao, J. Sun, S. Wang, H. Zhou, A Two-Stream End-To-End Deep Learning Network for Recognizing Atypical Visual Attention in Autism Spectrum Disorder, 2019 arXiv preprint arXiv:1911.11393.
- [183] M.I.U. Haque, D. Valles, Facial expression recognition from different angles using DCNN for children with ASD to identify emotions, in: 2018 International Conference on Computational Science and Computational Intelligence (CSCI), IEEE, 2018, December, pp. 446–449.
- [184] S. Sadiq, M. Castellanos, J. Moffitt, M.L. Shyu, L. Perry, D. Messinger, Deep learning based multimedia data mining for autism spectrum disorder (ASD) diagnosis, in: 2019 International Conference on Data Mining Workshops (ICDMW), IEEE, 2019, November, pp. 847–854.
- [185] M.I.U. Haque, D. Valles, Facial expression recognition using DCNN and development of an iOS app for children with ASD to enhance communication abilities, in: 2019 IEEE 10th Annual Ubiquitous Computing, Electronics & Mobile Communication Conference (UEMCN), IEEE, 2019, October, 0476–0482.
- [186] Y. Tao, M.I. Shyu, SP-ASDNet: CNN-LSTM based ASD classification model using observer scanpaths, in: 2019 IEEE International Conference on Multimedia & Expo Workshops (ICMEW), IEEE, 2019, July, pp. 641–646.
- [187] J.R.H. Lee, A. Wong, TimeConvNets: a deep time windowed convolution neural network design for real-time video facial expression recognition, in: 2020 17th Conference on Computer and Robot Vision (CRV), IEEE, 2020, May, pp. 9–16.
- [188] A. Vijayan, S. Janmasree, C. Keerthana, L.B. Syla, A framework for intelligent learning assistant platform based on cognitive computing for children with autism spectrum disorder, in: 2018 International CET Conference on Control, Communication, and Computing (IC4), IEEE, 2018, July, pp. 361–365.
- [189] A. Di Nuovo, D. Conti, G. Trubia, S. Buono, S. Di Nuovo, Deep learning systems for estimating visual attention in robot-assisted therapy of children with autism and intellectual disability, *Robotics* 7 (2) (2018) 25.
- [190] N.M. Rad, S.M. Kia, C. Zarbo, T. van Laarhoven, G. Jurman, P. Venuti, C. Furlanello, Deep learning for automatic stereotypical motor movement detection using wearable sensors in autism spectrum disorders, *Signal Process.* 144 (2018) 180–191.
- [191] S. Jaiswal, M.F. Valstar, A. Gillott, D. Daley, Automatic detection of ADHD and ASD from expressive behaviour in RGBD data, in: 2017 12th IEEE International Conference on Automatic Face & Gesture Recognition (FG 2017), IEEE, 2017, May, pp. 762–769.
- [192] Y.S. Liu, C.P. Chen, S.S.F. Gau, C.C. Lee, April, Learning lexical coherence representation using LSTM forget gate for children with autism spectrum disorder during story-telling, in: 2018 IEEE International Conference on Acoustics, Speech and Signal Processing (ICASSP), IEEE, 2018, pp. 6029–6033.
- [193] J. Li, Y. Zhong, J. Han, G. Ouyang, X. Li, H. Liu, Classifying ASD children with LSTM based on raw videos, *Neurocomputing* 390 (2020) 226–238.
- [194] W. Wei, Z. Liu, L. Huang, A. Nebout, O. Le Meur, Saliency prediction via multi-level features and deep supervision for children with autism spectrum disorder, in: 2019 IEEE International Conference on Multimedia & Expo Workshops (ICMEW), IEEE, 2019, July, pp. 621–624.
- [195] C. Wu, S. Liaqat, S.C. Cheung, C.N. Chuah, S. Ozonoff, Predicting autism diagnosis using image with fixations and synthetic saccade patterns, in: 2019 IEEE International Conference on Multimedia & Expo Workshops (ICMEW), IEEE, 2019, July, pp. 647–650.
- [196] S. Raj, S. Masood, Analysis and detection of autism spectrum disorder using machine learning techniques, *Procedia Computer Science* 167 (2020) 994–1004.
- [197] M. Elbattah, R. Carette, G. Dequin, J.L. Guérin, F. Cilia, Learning clusters in autism spectrum disorder: image-based clustering of eye-tracking scanpaths with deep autoencoder, in: 2019 41st Annual International Conference of the IEEE Engineering in Medicine and Biology Society (EMBC), IEEE, 2019, July, pp. 1417–1420.
- [198] O. Rudovic, Y. Utsumi, J. Lee, J. Hernandez, E.C. Ferrer, B. Schuller, R.W. Picard, October, Culturenet: a deep learning approach for engagement intensity estimation from face images of children with autism, in: 2018 IEEE/RSJ International Conference on Intelligent Robots and Systems (IROS), IEEE, 2018, pp. 339–346.
- [199] A. Cook, B. Mandal, D. Berry, M. Johnson, Towards automatic screening of typical and atypical behaviors in children with autism, in: 2019 IEEE International Conference on Data Science and Advanced Analytics (DSAA), IEEE, 2019, October, pp. 504–510.
- [200] H. Javed, C.H. Park, Behavior-based risk detection of autism spectrum disorder through child-robot interaction, in: Companion of the 2020 ACM/IEEE International Conference on Human-Robot Interaction, 2020, March, pp. 275–277.
- [201] K. Sun, L. Li, L. Li, N. He, J. Zhu, Spatial attentional bilinear 3D convolutional network for video-based autism spectrum disorder detection, in: ICASSP 2020-2020 IEEE International Conference on Acoustics, Speech and Signal Processing (ICASSP), IEEE, 2020, May, pp. 3387–3391.
- [202] H. Wang, L. Li, L. Chi, Z. Zhao, Autism screening using deep embedding representation, in: International Conference on Computational Science, Springer, Cham, 2019, June, pp. 160–173.
- [203] M.F. Misman, A.A. Samah, F.A. Ezudin, H.A. Majid, Z.A. Shah, H. Hashim, M. F. Harun, Classification of adults with autism spectrum disorder using deep neural network, in: 2019 1st International Conference on Artificial Intelligence and Data Sciences (AiDAS), IEEE, 2019, September, pp. 29–34.
- [204] Y. Fang, H. Duan, F. Shi, X. Min, G. Zhai, Identifying children with autism spectrum disorder based on gaze-following, in: 2020 IEEE International Conference on Image Processing (ICIP), IEEE, 2020, October, pp. 423–427.
- [205] R. Lahiri, M. Kumar, S. Bishop, S. Narayanan, Learning domain invariant representations for child-adult classification from speech, in: ICASSP 2020-2020 IEEE International Conference on Acoustics, Speech and Signal Processing (ICASSP), IEEE, 2020, May, pp. 6749–6753.
- [206] D.N. Fernández, F.B. Porras, R.H. Gilman, M.V. Mondonedo, P. Sheen, M. Zimic, A Convolutional Neural Network for Gaze Preference Detection: A Potential Tool

- for Diagnostics of Autism Spectrum Disorder in Children, 2020 arXiv preprint arXiv:2007.14432.
- [207] F.C. Tamilarasi, J. Shanmugam, Convolutional neural network based autism classification, in: 2020 5th International Conference on Communication and Electronics Systems (ICCES), IEEE, 2020, June, pp. 1208–1212.
- [208] M. Eni, I. Dinstein, M. Ilan, I. Menashe, G. Meiri, Y. Zigel, Estimating autism severity in young children from speech signals using a deep neural network, *IEEE Access* 8 (2020) 139489–139500.
- [209] B. Penchina, A. Sundaresan, S. Cheong, A. Martel, Deep LSTM recurrent neural network for anxiety classification from EEG in adolescents with autism, in: International Conference on Brain Informatics, Springer, Cham, 2020, September, pp. 227–238.
- [210] A. Sundaresan, B. Penchina, S. Cheong, V. Grace, A. Valero-Cabré, A. Martel, Evaluating deep learning EEG-based mental stress classification in adolescents with autism for breathing entrainment BCI, *Brain Informatics* 8 (1) (2021) 1–12.
- [211] N.M. Rad, S.M. Kia, C. Zarbo, T. van Laarhoven, G. Jurman, P. Venuti, C. Furlanello, Deep learning for automatic stereotypical motor movement detection using wearable sensors in autism spectrum disorders, *Signal Process.* 144 (2018) 180–191.
- [212] S. Ibrahim, R. Djemal, A. Alsuwailem, Electroencephalography (EEG) signal processing for epilepsy and autism spectrum disorder diagnosis, *Biocybernetics and Biomedical Engineering* 38 (1) (2018) 16–26.
- [213] R. Lajiness-O'Neill, A.E. Richard, J.E. Moran, A. Olszewski, L. Pawluk, D. Jacobson, S.M. Bowyer, Neural synchrony examined with magnetoencephalography (MEG) during eye gaze processing in autism spectrum disorders: preliminary findings, *J. Neurodev. Disord.* 6 (1) (2014) 1–22.
- [214] W. Sun, X. Wu, T. Zhang, F. Lin, H. Sun, J. Li, Narrowband resting-state fNIRS functional connectivity in autism spectrum disorder, *Front. Hum. Neurosci.* 15 (2021) 294.
- [215] D. Yang, Y.I. Shin, K.S. Hong, Systemic review on transcranial electrical stimulation parameters and EEG/fNIRS features for brain diseases, *Front. Neurosci.* 15 (2021) 274.
- [216] B.A. Cocui, S. Das, L. Billeci, W. Jamal, K. Maharatna, S. Calderoni, F. Muratori, Multimodal functional and structural brain connectivity analysis in autism: a preliminary integrated approach with EEG, fMRI, and DTI, *IEEE Transactions on Cognitive and Developmental Systems* 10 (2) (2017) 213–226.
- [217] R.R. Federico, A Study on Cerebral Activity by Means of Combined EEG-fMRI in Neuropsychological Disorders in Childhood, 2011.
- [218] C. O'Reilly, J.D. Lewis, M. Elsabbagh, Is functional brain connectivity atypical in autism? A systematic review of EEG and MEG studies, *PLoS One* 12 (5) (2017), e0175870.
- [219] J.I. Berman, J.C. Edgar, L. Blaskey, E.S. Kuschner, S.E. Levy, M. Ku, T.P. Roberts, Multimodal diffusion-MRI and MEG assessment of auditory and language system development in autism spectrum disorder, *Front. Neuroanat.* 10 (2016) 30.
- [220] L.E. Libero, T.P. DeRamus, A.C. Lahti, G. Deshpande, R.K. Kana, Multimodal neuroimaging based classification of autism spectrum disorder using anatomical, neurochemical, and white matter correlates, *Cortex* 66 (2015) 46–59.
- [221] C. Lord, E. Petkova, V. Hus, W. Gan, F. Lu, D.M. Martin, S. Risi, A multisite study of the clinical diagnosis of different autism spectrum disorders, *Arch. Gen. Psychiatr.* 69 (3) (2012) 306–313.
- [222] L.M. Oberman, A. Rotenberg, A. Pascual-Leone, Use of transcranial magnetic stimulation in autism spectrum disorders, *J. Autism Dev. Disord.* 45 (2) (2015) 524–536.
- [223] A. Amatachaya, N. Auvichayapat, N. Patjanasoontorn, C. Suphakunpinyo, N. Ngernyam, B. Aree-Uea, P. Auvichayapat, Effect of anodal transcranial direct current stimulation on autism: a randomized double-blind crossover trial, *Behav. Neurol.* 2014 (2014).
- [224] G. D'Urso, D. Buzzese, R. Ferrucci, A. Priori, A. Pascotto, S. Galderisi, C. Bravaccio, Transcranial direct current stimulation for hyperactivity and noncompliance in autistic disorder, *World J. Biol. Psychiatr.* 16 (5) (2015) 361–366.
- [225] A. İşin, C. Direkoglu, M. Şah, Review of MRI-based brain tumor image segmentation using deep learning methods, *Procedia Computer Science* 102 (2016) 317–324.
- [226] W. Li, X. Lin, X. Chen, Detecting Alzheimer's disease Based on 4D fMRI: an exploration under deep learning framework, *Neurocomputing* 388 (2020) 280–287.
- [227] K.K. Hyde, M.N. Novack, N. LaHaye, C. Parlett-Pelleriti, R. Anden, D.R. Dixon, E. Linstead, Applications of supervised machine learning in autism spectrum disorder research: a review, *Review Journal of Autism and Developmental Disorders* 6 (2) (2019) 128–146.
- [228] D.Y. Song, C.C. Topriceanu, D.C. Ilie-Ablachim, M. Kinali, S. Bisdas, Machine learning with neuroimaging data to identify autism spectrum disorder: a systematic review and meta-analysis, *Neuroradiology* (2021) 1–16.
- [229] M. Hosseinzadeh, J. Koohpayehzadeh, A.O. Bali, F.A. Rad, A. Souri, A. Mazaherinezhad, M. Bohloli, A review on diagnostic autism spectrum disorder approaches based on the Internet of Things and Machine Learning, *J. Supercomput.* 77 (3) (2021) 2590–2608.
- [230] M. Rahman, O.L. Usman, R.C. Muniyandi, S. Sahran, S. Mohamed, R.A. Razak, A Review of machine learning methods of feature selection and classification for autism spectrum disorder, *Brain Sci.* 10 (12) (2020) 949.
- [231] A.M. Pagnozzi, E. Conti, S. Calderoni, J. Fripp, S.E. Rose, A systematic review of structural MRI biomarkers in autism spectrum disorder: a machine learning perspective, *Int. J. Dev. Neurosci.* 71 (2018) 68–82.
- [232] M. Xu, V. Calhoun, R. Jiang, W. Yan, J. Sui, Brain imaging-based machine learning in autism spectrum disorder: methods and applications, *J. Neurosci. Methods* (2021) 109271.
- [233] S. Dedgaonkar, R. Sachdeo-Bedi, September). Technology support for autistic people: a survey, in: 2019 5th International Conference on Computing, Communication, Control and Automation (ICCCBEA), IEEE, 2019, pp. 1–5.
- [234] P. Soyaonkar, B. Patil, November). A survey: strategies for detection of autism syndrome disorder, in: 2020 IEEE 15th International Conference on Industrial and Information Systems (ICIIS), IEEE, 2020, pp. 449–454.
- [235] K.S. Kumar, K. Bairavi, IoT based health monitoring system for autistic patients, in: Proceedings of the 3rd International Symposium on Big Data and Cloud Computing Challenges (ISBCC–16'), Springer, Cham, 2016, pp. 371–376.
- [236] S. Golestan, P. Soleiman, H. Moradi, A Comprehensive Review of Technologies Used for Screening, Assessment, and Rehabilitation of Autism Spectrum Disorder, 2018 arXiv preprint arXiv:1807.10986.
- [237] M.S. Jaliaawala, R.A. Khan, Can autism be catered with artificial intelligence-assisted intervention technology? A comprehensive survey, *Artif. Intell. Rev.* 53 (2) (2020) 1039–1069.
- [238] A. Shoeibi, N. Ghassemi, M. Khodatars, P. Moridian, R. Alizadehsani, A. Zare, J. M. Gorri, Detection of Epileptic Seizures on EEG Signals Using ANFIS Classifier, Autoencoders and Fuzzy Entropies, 2021 arXiv preprint arXiv:2109.04364.
- [239] A. Shoeibi, D. Sadeghi, P. Moridian, N. Ghassemi, J. Heras, R. Alizadehsani, J. M. Gorri, Automatic Diagnosis of Schizophrenia Using EEG Signals and CNN-LSTM Models, 2021 arXiv preprint arXiv:2109.01120.
- [240] F. Khozeimeh, D. Sharifrazi, N.H. Izadi, J.H. Joloudari, A. Shoeibi, R. Alizadehsani, S.M.S. Islam, Combining a convolutional neural network with autoencoders to predict the survival chance of COVID-19 patients, *Sci. Rep.* 11 (1) (2021) 1–18.
- [241] R. Alizadehsani, D. Sharifrazi, N.H. Izadi, J.H. Joloudari, A. Shoeibi, J.M. Gorri, U.R. Acharya, Uncertainty-aware Semi-supervised Method Using Large Unlabelled and Limited Labeled COVID-19 Data, 2021 arXiv preprint arXiv: 2102.06388.
- [242] D. Sadeghi, A. Shoeibi, N. Ghassemi, P. Moridian, A. Khadem, R. Alizadehsani, S. Nahavandi, An Overview on Artificial Intelligence Techniques for Diagnosis of Schizophrenia Based on Magnetic Resonance Imaging Modalities: Methods, Challenges, and Future Works, 2021 arXiv preprint arXiv:2103.03081.
- [243] R. Alizadehsani, M. Roshanzamir, S. Hussain, A. Khosravi, A. Kohestani, M. H. Zangooei, U.R. Acharya, Handling of uncertainty in medical data using machine learning and probability theory techniques: a review of 30 years (1991–2020), *Ann. Oper. Res.* (2021) 1–42.
- [244] X.A. Bi, Y. Wang, Q. Shu, Q. Sun, Q. Xu, Classification of autism spectrum disorder using random support vector machine cluster, *Front. Genet.* 9 (2018) 18.
- [245] L. Squarcina, G. Nosari, R. Marin, U. Castellani, M. Bellani, C. Bonivento, P. Brambilla, Automatic classification of autism spectrum disorder in children using cortical thickness and support vector machine, *Brain and behavior* (2021).
- [246] M. Mohammadpoor, A. Shoeibi, H. Shojaee, A hierarchical classification method for breast tumor detection, *Iranian Journal of Medical Physics* 13 (4) (2016) 261–268.
- [247] N. Ghassemi, A. Shoeibi, M. Khodatars, J. Heras, A. Rahimi, A. Zare, J.M. Gorri, Automatic Diagnosis of COVID-19 from CT Images Using CycleGAN and Transfer Learning, 2021 arXiv preprint arXiv:2104.11949.
- [248] M. Baygin, S. Dogan, T. Tunçer, P.D. Barua, O. Faust, N. Arunkumar, U. R. Acharya, Automated ASD detection using hybrid deep lightweight features extracted from EEG signals, *Comput. Biol. Med.* 134 (2021) 104548.
- [249] D. Maheshwari, S.K. Ghosh, R.K. Tripathy, M. Sharma, U.R. Acharya, Automated accurate emotion recognition system using rhythm-specific deep convolutional neural network technique with multi-channel EEG signals, *Comput. Biol. Med.* 134 (2021) 104428.
- [250] D.S. Andrews, J.K. Lee, M. Solomon, S.J. Rogers, D.G. Amaral, C.W. Nordahl, A diffusion-weighted imaging tract-based spatial statistics study of autism spectrum disorder in preschool-aged children, *J. Neurodev. Disord.* 11 (1) (2019) 1–12.
- [251] C. Lord, M. Elsabbagh, G. Baird, J. Veenstra-Vanderweele, Autism spectrum disorder, *Lancet* 392 (10146) (2018) 508–520.
- [252] X. Dong, Y. Lei, S. Tian, T. Wang, P. Patel, W.J. Curran, X. Yang, Synthetic MRI-aided multi-organ segmentation on male pelvic CT using cycle consistent deep attention network, *Radiother. Oncol.* 141 (2019) 192–199.
- [253] Y. Yang, N. Wang, H. Yang, J. Sun, Z. Xu, Model-Driven deep attention network for ultra-fast compressive sensing MRI guided by cross-contrast MR image, in: International Conference on Medical Image Computing and Computer-Assisted Intervention, Springer, Cham, 2020, October, pp. 188–198.
- [254] T.M. Quan, T. Nguyen-Duc, W.K. Jeong, Compressed sensing MRI reconstruction using a generative adversarial network with a cyclic loss, *IEEE Trans. Med. Imag.* 37 (6) (2018) 1488–1497.
- [255] X. Yi, E. Walia, P. Babyn, Generative adversarial network in medical imaging: a review, *Med. Image Anal.* 58 (2019) 101552.
- [256] K. Han, Y. Wang, H. Chen, X. Chen, J. Guo, Z. Liu, D. Tao, A Survey on Visual Transformer, 2020 arXiv preprint arXiv:2012.12556.
- [257] A. Hering, S. Kuckertz, S. Heldmann, M.P. Heinrich, Memory-efficient 2.5 D convolutional transformer networks for multi-modal deformable registration with weak label supervision applied to whole-heart CT and MRI scans, *International journal of computer assisted radiology and surgery* 14 (11) (2019) 1901–1912.
- [258] O. Vinyals, C. Blundell, T. Lillicrap, K. Kavukcuoglu, D. Wierstra, Matching Networks for One Shot Learning, 2016 arXiv preprint arXiv:1606.04080.

- [259] A.M. Hafiz, S.A. Parah, R.U.A. Bhat, Attention Mechanisms and Deep Learning for Machine Vision: A Survey of the State of the Art, 2021 arXiv preprint arXiv: 2106.07550.
- [260] N.Q. Pham, T.S. Nguyen, J. Niehues, M. Müller, S. Stüker, A. Waibel, Very Deep Self-Attention Networks for End-To-End Speech Recognition, 2019 arXiv preprint arXiv:1904.13377.
- [261] Z. Niu, G. Zhong, H. Yu, A review on the attention mechanism of deep learning, *Neurocomputing* 452 (2021) 48–62.
- [262] T. Chen, X. Li, H. Yin, J. Zhang, June). Call attention to rumors: deep attention based recurrent neural networks for early rumor detection, in: Pacific-asia Conference on Knowledge Discovery and Data Mining, Springer, Cham, 2018, pp. 40–52.
- [263] G. Xue, S. Liu, Y. Ma, A hybrid deep learning-based fruit classification using attention model and convolution autoencoder, *Complex & Intelligent Systems* (2020) 1–11.
- [264] S. Genc, S. Mallya, S. Bodapati, T. Sun, Y. Tao, Zero-shot Reinforcement Learning with Deep Attention Convolutional Neural Networks, 2020 arXiv preprint arXiv: 2001.00605.
- [265] J. Bai, B. Ding, Z. Xiao, L. Jiao, H. Chen, A.C. Regan, Hyperspectral image classification based on deep attention graph convolutional network, *IEEE Trans. Geosci. Rem. Sens.* (2021).
- [266] G. Ghiasi, Y. Cui, A. Srinivas, R. Qian, T.Y. Lin, E.D. Cubuk, B. Zoph, Simple copy-paste is a strong data augmentation method for instance segmentation, in: Proceedings of the IEEE/CVF Conference on Computer Vision and Pattern Recognition, 2021, pp. 2918–2928.
- [267] A. Vaswani, N. Shazeer, N. Parmar, J. Uszkoreit, L. Jones, A.N. Gomez, I. Polosukhin, Attention is all you need, in: Advances in Neural Information Processing Systems, 2017, pp. 5998–6008.
- [268] S. Yun, M. Jeong, R. Kim, J. Kang, H.J. Kim, Graph transformer networks, *Adv. Neural Inf. Process. Syst.* 32 (2019) 11983–11993.
- [269] Q. Zhang, C. Bai, Z. Chen, P. Li, H. Yu, S. Wang, H. Gao, Deep learning models for diagnosing spleen and stomach diseases in smart Chinese medicine with cloud computing, *Concurrency Comput. Pract. Ex.* 33 (7) (2021), 1–1.
- [270] K. Zhang, The design of regional medical cloud computing information platform based on deep learning, *International Journal of System Assurance Engineering and Management* (2021) 1–8.
- [271] J. Vicnesh, J.K.E. Wei, S.L. Oh, N. Arunkumar, E. Abdulhay, E.J. Ciaccio, U. R. Acharya, Autism spectrum disorder diagnostic system using HOS bispectrum with EEG signals, *Int. J. Environ. Res. Publ. Health* 17 (3) (2020) 971.
- [272] S. Bhat, U.R. Acharya, H. Adeli, G.M. Bairy, A. Adeli, Automated diagnosis of autism: in search of a mathematical marker, *Rev. Neurosci.* 25 (6) (2014) 851–861.
- [273] S.L. Oh, V. Jahmunah, N. Arunkumar, E.W. Abdulhay, R. Gururajan, N. Adib, U. R. Acharya, A novel automated autism spectrum disorder detection system, *Complex & Intelligent Systems* (2021) 1–15.